December 2018/January 2019
Volume 124
Issue 1989
£5.90

www.electronicsworld.co.uk

Electronics WORLD

THE ESSENTIAL ELECTRONICS ENGINEERING MAGAZINE

Special Report on RF Design:

Structural design of a space active phased array antenna

INSIDE THIS ISSUE

T&M Supplement

- New applications drive increased accuracy in power measurement

Feature

- Ultra-wideband calibration-free 6-bit 4Gsps folding-interpolating ADCs

Feature

- Scanning acoustic microscopy from the lab to the high-throughput fab

ALSO IN THIS ISSUE:

Latest Products:
* Signal generators
* Current sensors
* Power supplies

Have confidence in your measurement

Whether you need calibration for existing or new test and measurement instruments, it's important you can trust your equipment.

Our expert UKAS-accredited laboratory offers a fast turnaround calibration service for brand new equipment and a re-calibration service to fine-tune your existing tools.

Find out more

uk.rs-online.com/services

CONTENTS

REGULARS

COLUMNS

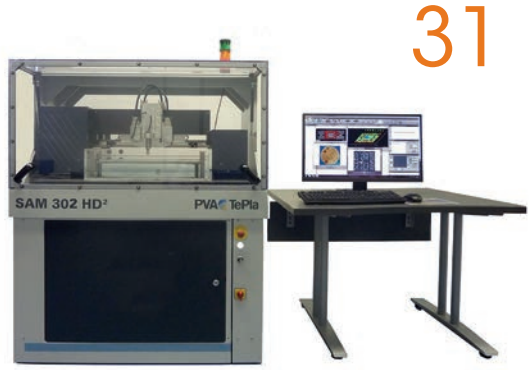

FEATURES

T&M SUPPLEMENT

A YEAR IN THE LIFE OF BLUETOOTH MESH

Over two decades, Bluetooth technology has revolutionised the IoT market, adding new capabilities, aiding innovation and establishing new markets – from wireless audio to connected devices.

In 2018, the Bluetooth Special Interest Group (SIG) celebrates its 20th anniversary. Formed in 1998, the group started with just a handful of companies, looking to replace the tangle of cables commonly used to communicate between devices with a wireless alternative. Today, the membership counts over 34,000 companies.

Part of that continuing expansion is due to Bluetooth mesh networking, a major enhancement to the Bluetooth standard, introduced in July 2017. This technology enables many-to-many (m:m) device communications and is optimised for creating large-scale device networks.

Designed to meet the scaleability, reliability and security requirements of commercial and industrial environments, Bluetooth mesh powers smart building and smart industry implementations where up to tens of thousands of devices must communicate effectively.

Today, many buildings are not that well integrated – lacking a networking system that allows organisations to monitor and control their lights and other systems, using sensors that inform them in real time what they should and shouldn't be doing. With a mesh network in place, a building becomes self-optimising environment that reduces costs and improves conditions for its users.

From factories to hospitals, airports, retail stores and the home, Bluetooth mesh supports building services that bring real value to owners, operators and occupants, and is already playing a pivotal role in the development of emerging markets such as smart buildings, smart industry, smart cities and smart homes.

The Bluetooth Qualification Process ensures that all Bluetooth products achieve global interoperability. It also gives the Bluetooth SIG visibility into the types of products being developed, offering insights into market trends, and affording a unique perspective on the adoption of Bluetooth technologies.

There are now 65 qualified Bluetooth products with mesh networking capability, with this number growing fast.

Upon its release, it was widely believed that the technology's first adopter would be the smart-building market and, specifically, connected lighting solutions designed for commercial building automation. The forecasts have called it right, and lighting control systems have been a key example in driving the adoption of Bluetooth mesh.

A building's lighting system provides a natural grid through which all devices in a Bluetooth mesh network can pass messages and establish in-building control, monitoring and automation systems. This wireless lighting solution could also function as a platform to enable indoor positioning and location services – including point-of-interest solutions, indoor navigation, asset tracking and improved space utilisation.

As developments continue to lay the groundwork for the smart infrastructures of the future, chances are they will be connected by Bluetooth mesh

In a single year, Bluetooth mesh has paved the way for wireless lighting control solutions and has been a driving force in realising the concept of lighting as a platform. Though designed to meet the high demands of commercial and industrial markets, Bluetooth mesh easily scales down to meet the requirements of the smart-home market. So, it's no surprise that it has gained early traction in the smart home.

Lijuan Chen, Head of Alibaba A.I. Labs, which leads consumer AI product development at the Alibaba Group, said: "The strategic decision to adopt Bluetooth as the communications platform for our smart home strategy was an obvious choice for us. Bluetooth mesh is a wireless protocol that enables us to meet our customers' scale, performance and reliability requirements in the home."

ABI research predicts a 7x growth in annual shipments of Bluetooth smart industry devices by 2022, while annual volume of Bluetooth smart-home enabling devices are expected to increase by 5x over the same period.

As developments in the connected device market continue to lay the groundwork for the smart infrastructures of the future, chances are they will be connected by Bluetooth mesh. ❖

By Martin Woolley, Developer Relations Manager, EMEA, Bluetooth SIG (www.bluetooth.com)

EDITOR: Svetlana Josifovska
Tel: +44 (0)1732 883392
Email: svetlanaj@electronicsworld.co.uk

SALES: Suzie Pipe
Tel: +44 (0)20 8306 0564
Mobile: +44 (0)7799 063311
Email: suziep@electronicsworld.co.uk

GROUP SALES MANAGER: Sunny Nehru
Tel: +44 (0)20 7062 2539

DESIGN: Tania King

PUBLISHER: Wayne Darroch

SJP business media

2nd floor,
St Mary Abchurch House,
123 Cannon Street,
London,
EC4N 5AU

ISSN: 1365-4675
PRINTER: Buxton Press Ltd

SUBSCRIPTIONS:
Subscription rates:
UK - 1 year digital only £53.00+VAT
UK - 1 year print and digital sub £68.00
UK - 2 year print and digital sub £109.00
UK - 3 year print and digital sub £143.00
International - 1 year digital only £53.00
International - 1 year print and digital sub £164.00
International - 2 year print and digital sub £290.00
International - 3 year print and digital sub £409.00
Tel/Fax +44 (0)1635 879361/868594
Email: electronicsworld@circdata.com
www.electronicsworld.co.uk/subscribe

Follow us on Twitter @electrowo

Join us on LinkedIn

RESEARCH SHOWS THAT NANOMACHINE SWARMS COULD IMPROVE THE EFFICIENCY OF OTHER MACHINES

Nanotech researchers at the University of Luxembourg have found that nanomachines are far more efficient at converting one type energy into another compared to their larger counterparts, such as motors and other industrial machines, for example.

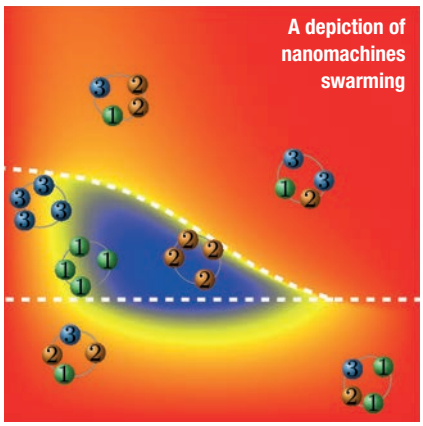

A depiction of nanomachines swarming

It's well known that all machines convert one form of energy into another; for example, a car engine turns the energy created by its fuel into motion. But, energy conversion, covered by the science of thermodynamics, takes place not only on the macro level in big machines, but also at the micro- and even nano-level of molecular machines that drive muscles or metabolic processes.

The research team led by Professor Massimiliano Esposito of the University of Luxembourg studies the thermodynamics of tiny nanomachines consisting of only a few atoms. Their insights will be used to improve the energy efficiency of all kinds of machines, big and small.

Recent progress in nanotechnology has enabled researchers to understand the world at ever-smaller scales and even design and manufacture extremely small machines.

"There is evidence that these machines are far more efficient than large machines, such as cars. Yet in absolute terms, their output is low compared to our needs in daily life applications," said Tim Herpich, PhD student at University's research group and main author of the paper. "That is why we studied how nanomachines interact with each other, and looked at how their ensembles behave. We wanted to see if there are synergies when they act together."

The researchers found that under certain conditions nanomachines start to arrange in swarms and synchronise their movements.

"We could show that the self-synchronisation of the machines triggers significant synergy, so that the overall energy output of the ensemble is far greater than the sum of the individual outputs," added Professor Esposito.

While this research is still at an early stage, its principles might be used to improve the efficiency of any machine in the future.

SCIENTISTS DEVELOP 'STAR TREK'-INSPIRED MEDICAL DIAGNOSTIC DEVICE

University of Glasgow researchers in the UK have developed a device that will help medics make quick and accurate diagnosis of a patient, not far off from the Star Trek's famous 'tricorder'.

The device pairs a handheld sensor with a smartphone app to measure levels of various molecules in fluid samples from patients. These molecules, known as "metabolites", depending on their abundance indicate the general heath or progression of specific diseases.

The ability to rapidly detect and quantify multiple metabolite biomarkers away from the lab makes this device particularly useful in cases of heart attack, cancer and stroke, where rapid diagnosis is vital for effective treatment. While metabolites can currently be measured by processes such as nuclear magnetic resonance and hyphenated mass spectrometry techniques, both approaches are expensive and require bulky equipment, which slow down the diagnostic results.

The device's CMOS-based chip is divided into multiple reaction zones to detect and quantify different metabolites simultaneously from body fluids such as serum. The device can be operated via any Android-based tablet or smartphone.

The Star Trek medical tricorder is now a step closer to real-life implementation

"Handheld, inexpensive diagnostic devices capable of accurately measuring metabolites open up a wide range of applications for medicine, and this latest development is an important step closer to bringing such a device to market," said Professor David Cumming, Principal Investigator of the project from Glasgow University's School of Engineering.

The project was funded by the Engineering and Physical Sciences Research Council (EPSRC).

Using digitisers as oscilloscopes

BY **OLIVER ROVINI** AND **GREG TATE**, SPECTRUM INSTRUMENTATION

"When can a digitiser be used as an oscilloscope and what is the difference between an oscilloscope digitiser and a non-oscilloscope digitiser?"

These are interesting questions, and the best way to start to answer them is to look up the dictionary definition of an oscilloscope: "An electronic instrument used to measure changing electric voltages. It displays the waveforms of electric oscillations on a screen".

A digitiser along with appropriate software can do the same thing – it acquires an electrical voltage waveform and displays it on a screen. The biggest difference is that an oscilloscope is generally a standalone instrument with a self-contained display, whereas a digitiser is a system component that acquires and stores an electrical voltage waveform and, with auxiliary software, displays that data on a screen. So, a digitiser can be used like an oscilloscope, which raises two further questions:

1. Why would you use a digitiser in place of an oscilloscope?
2. What digitiser characteristics make it a candidate for replacing an oscilloscope?

A Digitiser Instead of an Oscilloscope

One answer to the first question is that digitisers can support a greater number of input channels. Digitisers offer up to 16 channels for a single digitiser card, and some manufacturers' products allow up to 16 cards to be linked together, for a total of 256 channels. This is a major advantage over oscilloscopes, which are generally limited to fewer than eight channels per instrument.

Digitisers also offer multiple channels in a smaller package. Compare an eight-channel digitiser with an eight-channel oscilloscope and you will readily see the difference. The digitiser card is so small that it can plug directly into a vacant PCIe slot in most modern PCs. Digitisers also offer a considerable advantage, with their much lower power consumption for the same number of channels.

The next consideration is vertical resolution. Oscilloscopes offer a maximum of 8-12 bits of resolution, whereas in fast digitisers this is 8-16 bits. Keep in mind that resolution is bandwidth-dependent, so the comparison works between instruments of the same bandwidth.

If you need to move data with high throughput to a PC for processing, then a digitiser is the best choice. For example, digitisers can stream data at up to 3.4GB/s

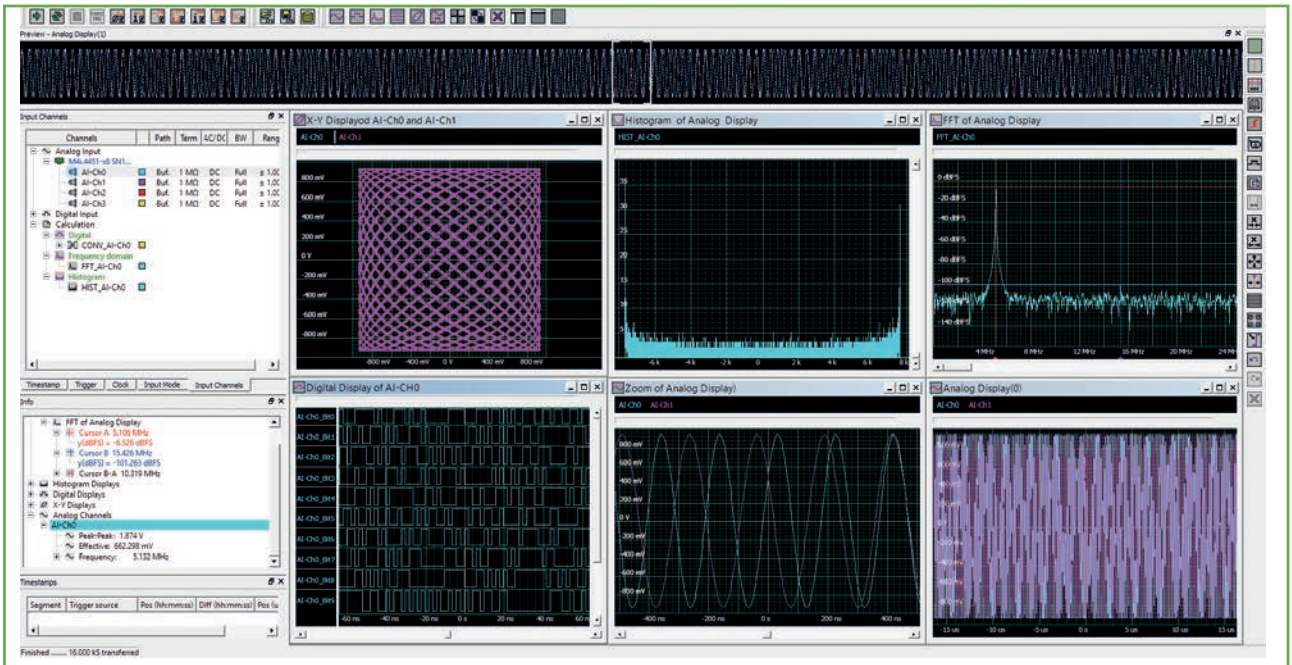

Figure 1: Software allows digitisers to operate like oscilloscopes to control, acquire, view, measure and analyse waveforms

over the PCIe bus, while standalone oscilloscopes normally use much slower interfaces like USB or LAN. This makes data from the digitiser available orders of magnitude faster than that from the oscilloscope. So, the digitiser is certainly the instrument of choice whenever customised signal processing and data analysis are required.

Another point for consideration is remote measurements. Network-based digitisers offer LXI control and data transfer, so the digitiser can be located a great distance from the measurement location. This is ideal if you need to view data and control an instrument from a lab, control room, office, or anywhere on your company's LAN.

The digitiser is also an expandable system component, since it is easy to increase the number of channels and change its configuration. Change or add cards and you can modify the available bandwidth, sampling rate and record length. In contrast, the oscilloscope is an instrument with a relatively fixed configuration; see Table 1 for comparisons.

A Digitiser Replacing an Oscilloscope

There are hundreds of digitiser models and configurations to choose from. Once you get past the basic questions of number of channels and the bandwidth, there are several more things to consider when selecting a digitiser to replace an oscilloscope.

The first is the sample rate: is it fixed or is there a selection of rates? Oscilloscopes offer selectable sample rates to view different frequency signals, and a digitiser replacing an oscilloscope should do the same. In general, the sample rate should be four to five times the bandwidth to accurately digitise waveforms with fast edges. Some digitisers offer a phase locked loop-based time-base that is programmable. Additionally, an external clock or external reference clock can be used to drive or synchronise the sampling rate with another source.

Acquisition memory determines the longest time record that can be acquired without reducing the sample rate. Digitisers can offer up to 4 giga-samples of memory as standard; that is about four times the maximum memory of a high-end oscilloscope. In practice, this means the digitiser can record longer waveforms without having to lower the sampling rate, and therefore lose valuable time resolution.

Digitisers used as an oscilloscope also need a flexible front-end configuration. For example, digitisers can offer both 50Ohm and 1MOhm inputs at their buffered input and a 50Ohm high-frequency input path with very high signal integrity. Both input paths offer multiple input ranges just like an oscilloscope.

Acquisition memory determines the longest time record that can be acquired without dropping the sample rate

Oscilloscopes offer real-time and segmented acquisition modes. Sequential mode allows the acquisition memory to be segmented and, for applications where multiple events are to be acquired, it can reduce the acquisition dead time (the re-arm time between events). Digitisers generally offer a number of different acquisition modes. For example, ring buffer mode (similar to an oscilloscope's real-time acquisition), FIFO or streaming mode, multiple recording (segmented mode), gated sampling and a multiple time base (ABA mode) that combines slow continuous recording with fast acquisition of trigger events. These multiple acquisition modes feature a fast re-arm time that can be as short as 80 sample periods (i.e. 16ns at 5GS/s). This is considerably shorter than the 1µs re-arm times of most oscilloscopes.

These different acquisition modes allow the user to configure the digitiser to best use its acquisition memory for different applications.

Triggering synchronises data acquisition with external events. Effective use of a digitiser requires great flexibility in device triggering. Simple edge triggers based on the slope and signal level are pretty standard on most digitisers; many offer window-triggering, as well.

Trigger sources include acquisition channels and multiple external trigger inputs. For maximum trigger flexibility, these inputs, along with re-arm capability, can be combined logically to produce advanced trigger states.

One of the key advantages of digitisers is their ability to rapidly stream data to a computer for further analysis and archiving. Some digitisers, in FIFO mode (streaming mode), are designed for continuous data transfer between their buffer memory and PC memory. Utilising a PCI Express x8 Gen 2 interface, streaming speed is up to 3.4GB/s. Oscilloscopes, mostly using LXI or USB interfaces, are considerably slower in their ability to move data to a computer. Combining the digitiser's streaming capability with a fast data storage system (like a RAID-based disc drive unit) makes the digitiser perfect for applications where long seamless waveforms need to be stored. Systems can easily be configured to allow hours or even days of continuous recording.

Software for Handling Data from Modular Digitisers

Digitisers are 'blind' instruments, normally without an integral display to view, measure or analyse the data they collect. Instead, these functions are usually performed by a PC.

Software is, therefore, needed to control the digitiser and view the waveforms acquired. It should perform both simple and complex measurements and offer multiple analysis tools. It should also allow the user to confirm the digitiser's operation during the development of their own custom software, and serve as an offline station for reviewing and analysing data.

Figure 1 shows the versatility of software in controlling, acquiring, viewing, measuring and analysing data with a digitiser, allowing it to be operated just like an oscilloscope. Here, two channels of data have been acquired and are shown in the lower-right grid. A horizontal expansion of that trace is shown in the lower-centre grid. The upper-left grid shows an X-Y plot of those two signals. The lower-left grid contains a digital display of the fourteen bits making up the signal on channel 1. The Fast Fourier transform (FFT) of the signal from channel 1 is shown in the upper-right display, while the upper-centre display shows the histogram of the same signal.

The software also provides cursors (two

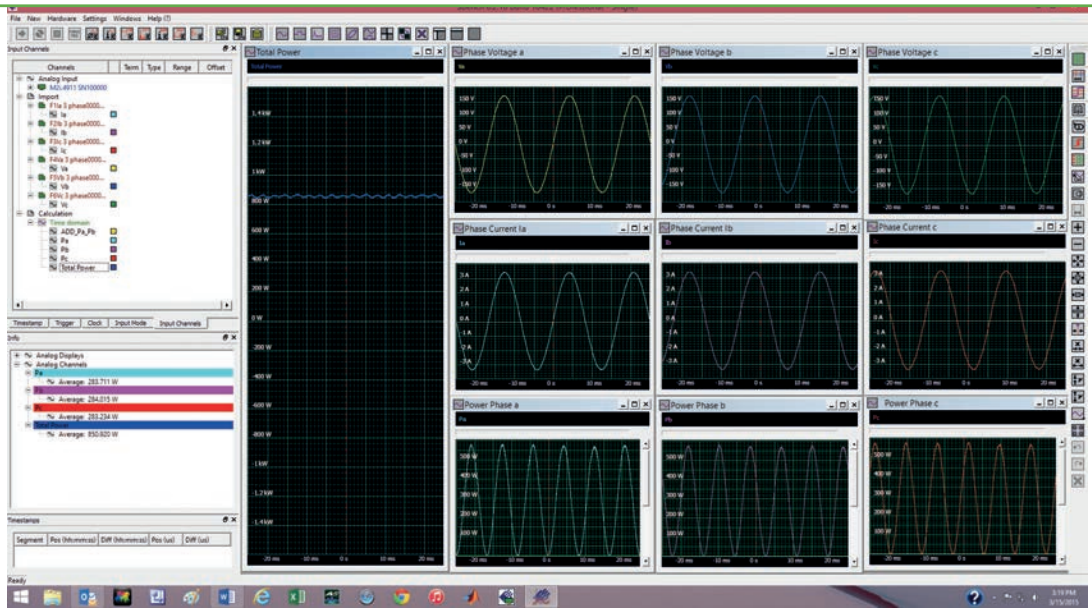

Figure 2: Computing the phase power using all three phase voltages and three phase currents for our simple example

for each display grid) and measurement parameters. Cursors are shown on the FFT display where the amplitude and frequency of the spectral lines at 5 and 15MHz are measured. The cursor readouts appear in the Info pane to the left of the figure associated with the FFT display.

Three of the 21 measurements are also shown in the Info pane associated with channel AI-Cho. These are the peak-to-peak amplitude, effective (rms) amplitude and frequency.

Analysis tools in the software include averaging, waveform arithmetic, FFT, histogram, filtering and conversion between analogue and digital domains.

Practical Measurement with a Digitiser as an Oscilloscope

In Figure 2, we show the phase voltages (V_a, V_b and Bc), phase currents (I_a, I_b and I_c), and phase power dissipation (P_a, P_b and P_c) for a WYE-connected load (where we have access to both the phase and line voltages).

Multiply each phase voltage by its related phase current and the result is the instantaneous power in each phase. The mean value of the instantaneous power is the real power component. The sum of all three phase power readings is the total real power of the load.

This measurement is referred to as the three-wattmeter power measurement. If we were to make this measurement using external differential probes to measure the voltages, it would require six channels. With single-ended probes the number of channels increases to nine. The flexibility of being able to specify up to 16 channels in a single digitiser card is a major advantage in this type of measurement.

The phase voltages are shown in the top row of Figure 2. Phase currents appear in the centre row. The waveforms are multiplied together using analogue calculations, with the resultant phase power appearing in the bottom row. The sum of all three phase power waveforms, again an analogue summation, appears in the leftmost grid labelled "Total Power". Note that the total power is relatively constant.

DIGITISER ADVANTAGES	*OSCILLOSCOPE ADVANTAGES*
Buy only what you need - from one to a large number of channels per system, expandable as needed.	*Higher overall bandwidth available (at a cost)*
Higher vertical resolution available at a given bandwidth	*Highly interactive viewing and control (touch screens, front panel controls)*
Small, compact, low power instrument	*Large number of compatible probes*
High data throughput	*Large number of built-in measurements and analysis techniques are available (at a cost)*
Lower cost per channel	
Customisable measurements and analysis (user-programmable and third-party software)	

Table 1: Comparing digitisers and oscilloscopes

Real-time calculations, shown in the Info pane on the left, show the average values of the individual phase power waveforms along with the total power. The sum of the average values of the three phase-power measurements equals the average total power, in this case 850.9W.

The Power of a Digitiser

These examples show the power in combining a digitiser with software to make measurements just like an oscilloscope.

Keep in mind the key advantages offered by the digitiser and your next 'oscilloscope' purchase might actually turn out to be a digitiser:

1. Larger maximum number of channels.
2. Lower cost and power use per channel.
3. Greater amplitude resolution at commensurate bandwidths.
4. Higher data throughput for faster automated measurements.
5. Smaller volume for equivalent number of channels.
6. Easy remote control.
7. Customised software and access to off-the-shelf analysis tools.
8. Modularity and expandability. ❖

FREE BOOKS

This article is adapted from *"The Digitizer Handbook – Precision and Performance in PC Instrumentation"* by Spectrum Instrumentation.

To receive a free copy, go to https://spectrum-instrumentation.com/en/contact-us and tick the box marked "Please send me a copy of the Digitizer Handbook" , adding "EW" in the Comment section.

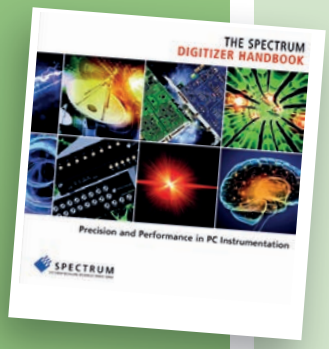

BY **DR MURAT UZAM**, ACADEMIC AND TECHNICAL AUTHOR, TURKEY

0-10V to 0-5V signal converter – analogue input modules

This series is dedicated to a project involving thirteen analogue input modules and seven analogue output modules, to be used with a 5V microcontroller via its ADC and DAC channels.

In previous columns we discussed 0-5V analogue input modules 1 to 5 that are fed DC input voltages from 0V to 6.26V, 12V and 24V, and requiring different DC power supplies.

In this month's column, we will focus on the sixth and seventh analogue input modules, the 0-10V to 0-5V signal converters – analogue input modules 1 and 2. Input module 1 and 2, can accept DC input voltages from 0V to 24V, and require two DC power supplies: 6.26V and 12V.

Analogue Input Module 1

Figure 1 shows the schematic of the 0-10V to 0-5V signal converter, analogue input module 1, with its connections shown in Figure 2. This design assumes that the input voltage range (V_{IN}) = 0.00V to 24V. When $0.00V \leq V_{IN} \leq 10.00V$, $V_{OUT} = V_{IN}/2$. When 10.02 V – VIN – 24V, V_{OUT} will be equal to a value from 5.01V to 5.07V, due to the characteristics of the LM358P-A.

The relationship between V_{OUT} and V_{IN} is shown in Figure 3. It can be seen that input voltage values up to 24V are accepted without damage to the circuit, and the output is a value from 5.01V to 5.07V.

Analogue voltage input signal V_{IN} can be subjected to electric surge or electrostatic discharge on the external terminal connections. The TVS (transient voltage suppressor) shown in the circuit provides highly effective protection against such discharges. D1 is used to protect the circuit from accidental reverse polarity of V_{IN}. A ferrite bead in series with the input path adds isolation and decoupling from high-frequency transient noises. Resistors R1 and R2 divide down the input signal V_{IN} into the range of 0V to 5V. External Schottky diodes generally protect the operational amplifier.

Even with internal ESD protection diodes, the use of external diodes lowers noise and offset errors. So, dual series Schottky barrier diodes D2 and D3 are there to divert any overcurrent to the power supply or ground.

The operational amplifier LM358P-A, with a +6.26V supply voltage, acts as a voltage limiter and is connected as a buffer amplifier (a voltage follower). V_{OUT} is obtained from the output of the LM358P-A.

Table 1 shows example input and output voltages for this module, with top and bottom views of the prototype circuit board in Figure 4.

It's worth noting that for proper operation make R1 = R2.

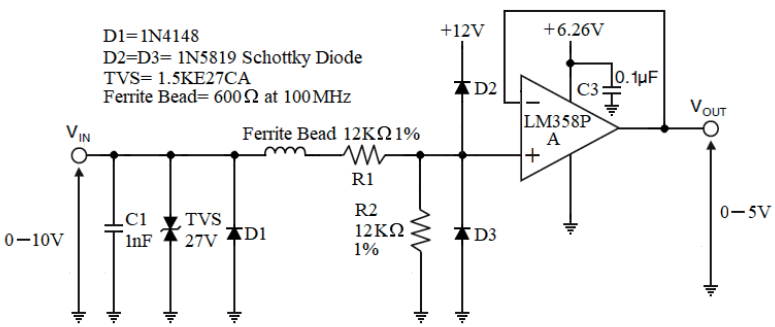

Figure 1: The schematic diagram of the 0-10V to 0-5V signal converter, analogue input module 1 for use with an ADC input of a 5V microcontroller

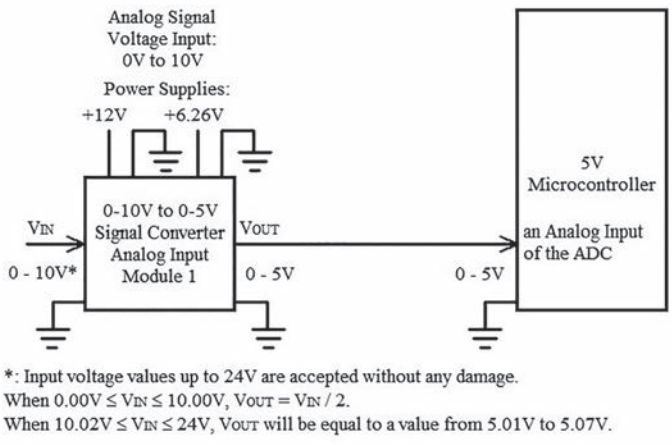

Figure 2: Connections of the 0-10V to 0-5V signal converter, analogue input module 1

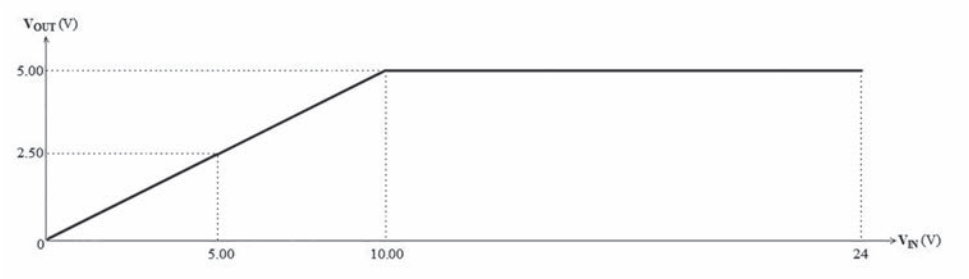

Figure 3: V_{OUT} vs V_{IN} for the 0-10V to 0-5V signal converter, analogue input modules 1 and 2

V_{IN}(V)	V_{OUT}(V)
24.00	5.0X
..	5.0X
20.00	5.0X
..	5.0X
10.00	5.00
..	..
9.00	4.50
..	..
8.00	4.00
..	..
7.00	3.50
..	..
6.00	3.00
..	..
5.00	2.50
..	..
4.00	2.00
..	..
3.00	1.50
..	..
2.00	1.00
..	..
1.00	0.50
..	..
0.00	0.00

Table 1: Example input and output voltage values forthe 0-10V to 0-5V signal converter, analogue input modules 1 and 2

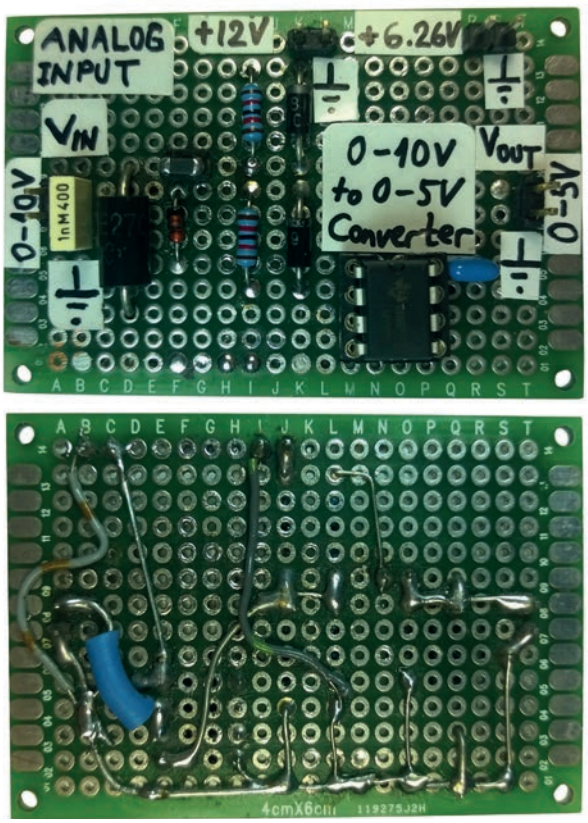

Figure 4: Top and bottom views of the prototype circuit board of the 0-10V to 0-5V signal converter, analogue input module 1

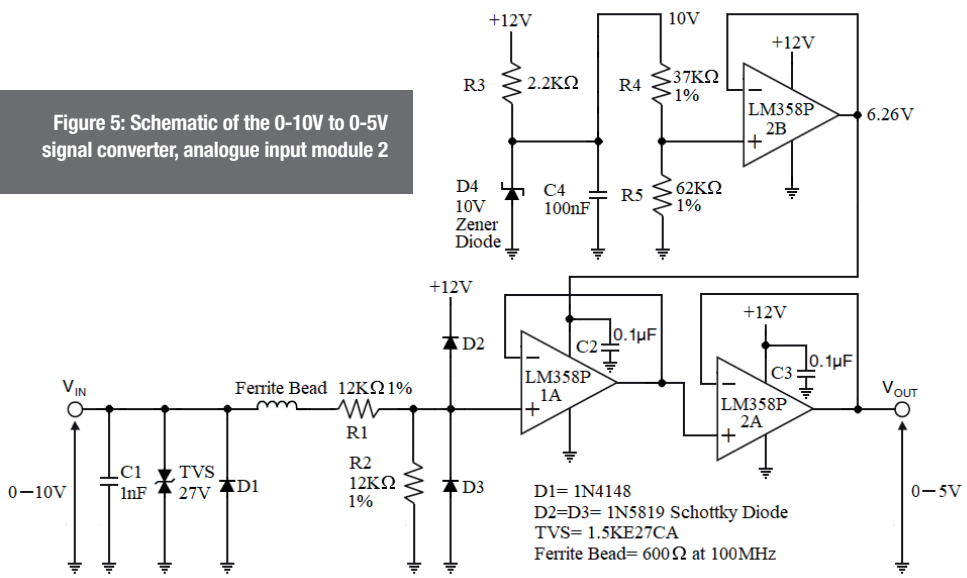

Figure 5: Schematic of the 0-10V to 0-5V signal converter, analogue input module 2

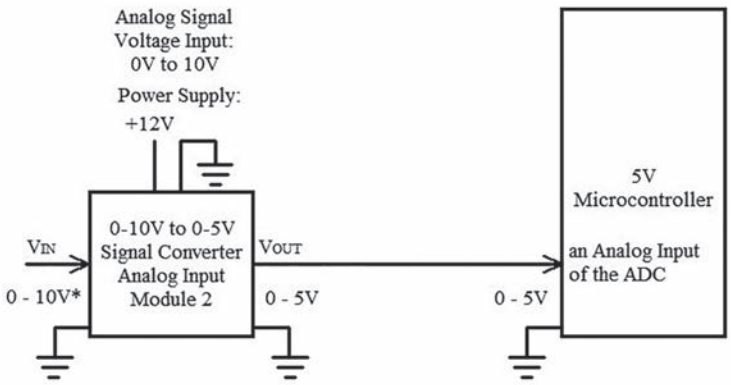

*: Input voltage values up to 24V are accepted without any damage.
When 0.00V ≤ VIN ≤ 10.00V, VOUT = VIN / 2.
When 10.02V ≤ VIN ≤ 24V, VOUT will be equal to a value from 5.01V to 5.07V.

Figure 6: Module 2's connections to the analogue input of a 5V microcontroller

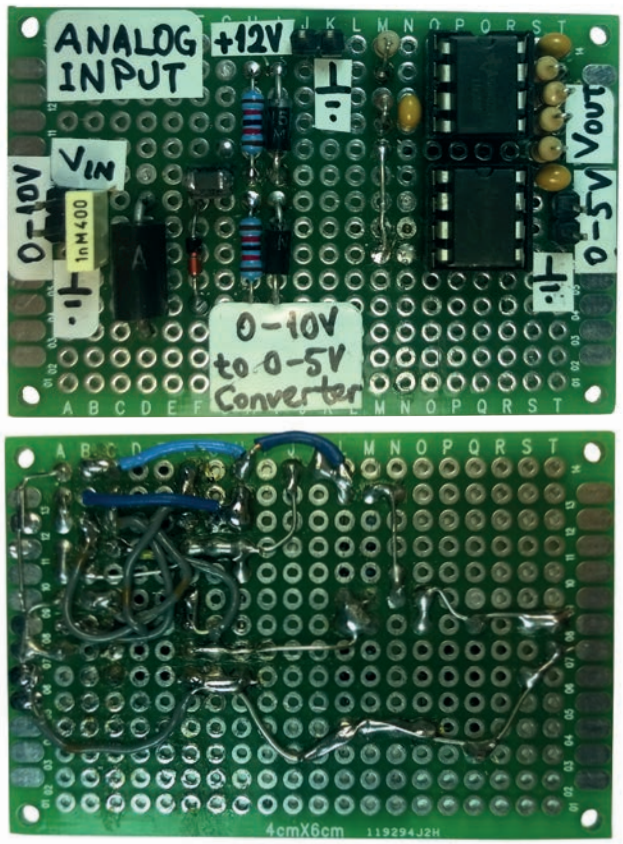

Figure 7: Top and bottom views of module 2's prototype circuit board

Analogue Input Module 2

Figure 5 shows the schematic of the 0-10V to 0-5V signal converter – analogue input module 2 for use with an ADC input of a 5V microcontroller; Figure 6 shows its connections. In this design, as in the previous module, it is assumed that the input voltage range (V_{IN}) = 0.00V to 24V. When 0.00V ≤ V_{IN} ≤ 10.00V, V_{OUT} = V_{IN}/2. When 10.02 V ≤ V_{IN} ≤ 24V, V_{OUT} will be from 5.01V to 5.07V, due to the characteristics of the LM358P-1A. The relationship between V_{OUT} and V_{IN} is shown in Figure 3.

Except for the buffer amplifier LM358P-2A, the source of the output voltage V_{OUT}, the lower part of the schematic diagram is identical with that of module 1's. The upper part produces the 6.26V reference voltage. R3, D4 (10V zener diode) and C4 provide a 10.00V reference voltage from the 12V power supply. Then, this 10.00V reference voltage is divided using resistors R4 and R5 to obtain a 6.26V reference voltage. This voltage is connected to the non-inverting input of the buffer amplifier LM358P-2B, whose output is fixed as a 6.26V reference voltage, capable of sourcing up to 20mA.

Table 1 shows example input and output voltage values for this module, with views of its prototype circuit in Figure 7.

For proper operation, be sure to make R1 = R2 and R5/(R4+R5) = 62.62%. ❖

This series continues in the next issue

PROTEUS DESIGN SUITE

Advanced PCB features for professional board design

DESIGN ROOMS

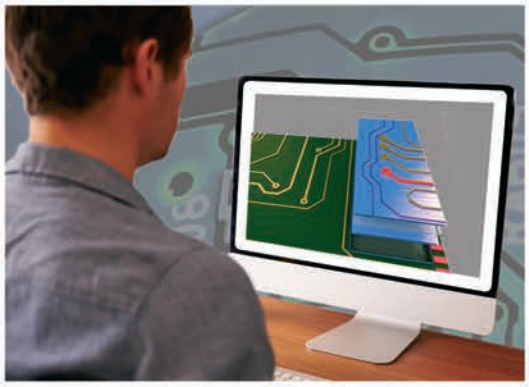

Set design rules that apply in user specified areas of the PCB.

LAYER STACKUP

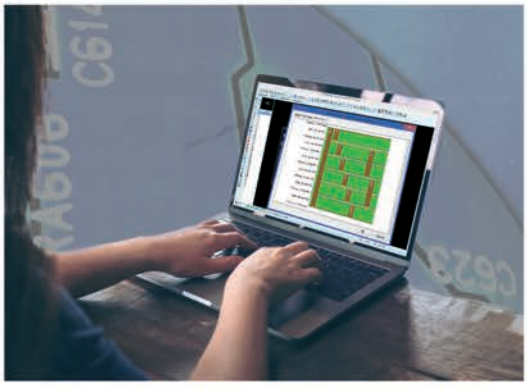

Control the layer stackup and drill ranges for smarter routing.

SERPENTINE ROUTING

Easily length match tracks against each other or to a target distance.

DESIGN VARIANTS

Edit the fitted status of parts or re-place with pin compatible alternatives.

The Proteus Design Suite provides advanced features at an affordable price. Try it today!

Visit: www.labcenter.com

Tel: +44 (0) 1756753440
E-Mail: info@labcenter.com
youtube.com/c/LabcenterElectronicsLtd

Labcenter Electronics www.labcenter.com

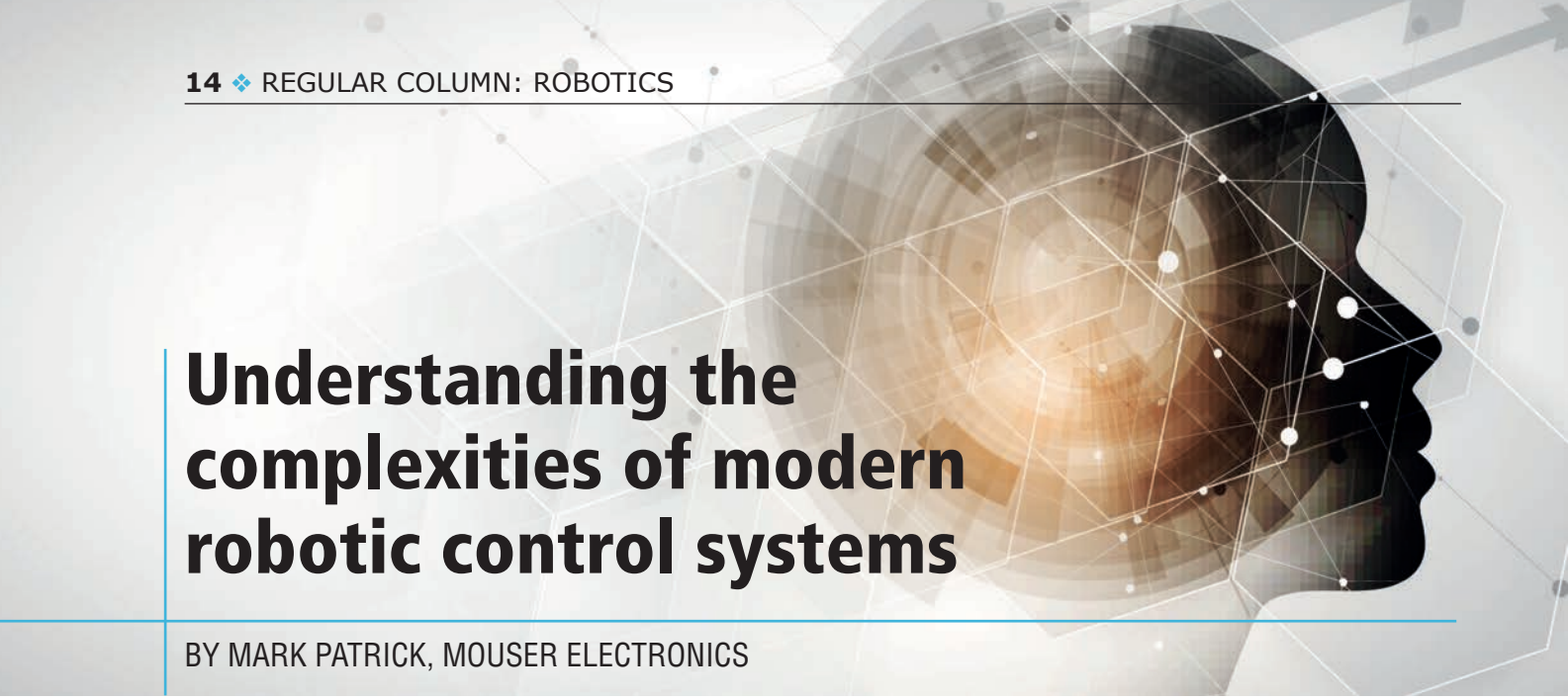

Understanding the complexities of modern robotic control systems

BY MARK PATRICK, MOUSER ELECTRONICS

Controlling the motion of modern robots often means managing movements along or around more than one axis. And while state-of-the-art electronics is making highly-precise motion control simpler to achieve, designers are also requiring more from these systems. The result is that motion-control remains a significant challenge.

Given the mechanical nature of robotics, part of the control loop will invariably need mechanical systems. These, however, bring with them vibrations, gear backlash, momentum, structural flexibility and many other problems. So, picking the right motor for the desired motion is essential: a brushless DC motor or stepper motor is typically best in low- or moderate-power scenarios.

Sensors

Knowing where the end effector is, as well as its speed and acceleration at any time, is extremely important, and normally requires a sensor, whether Hall-effect, optical encoder or synchro/resolver. For optimal accuracy, sometimes it is necessary to mount this sensor near the load endpoint, rather than on the motor.

Of course, some applications keep cost and complexity down by not using a sensor. This sensorless field-orientated control takes voltage and current readings at each phase of the motor windings and performs complex calculations to work out the position of the motor. The drawback is that this requires more computing power and more sophisticated programming. Moreover, this approach doesn't convey the same confidence or robustness as using a sensor. Consequently, sensors remain the preferred choice for many robotics designers.

Common Classifications of Robots

When hearing the word "robot", most would think of a human-like assistant that moves around freely. Most robotic systems in industry are rather different; they are stationary machines with arms set up to do specific tasks. Many can broadly be classified as cartesian, cylindrical or spherical robots:

- Cartesian robots (Figure 1) are easiest to control, since they move linearly along the x, y and z axes. They're typically used for applying sealants, simple assembly and pick-and-place.
- A cylindrical robot (Figure 2) provides motion along two linear axes, and rotational motion around one of them. This type is widely found in spot welding, handling tools or assembly work.

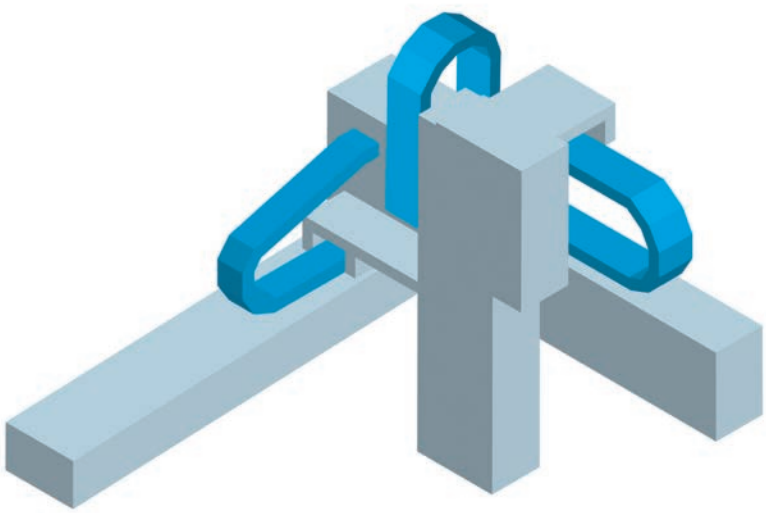

Figure 1: Cartesian robot

- Spherical robots (Figure 3) have a pair of rotary joints and a linear one, enabling them to operate in a spherical zone. They're used for welding, tool-handling and casting.

These setups give three degrees of freedom, but not all applications might need them all. Conversely, for those applications that need more than three, this can be achieved using multiple joints. The key challenge is that with added degrees of freedom, it becomes exponentially more difficult to control the robot smoothly and accurately.

Choosing a Trajectory Profile

When designing a control system for any robot, an important consideration is the profile of its movement trajectory. For example, getting the arm to its endpoint more quickly can be achieved by accelerating and decelerating faster at each end of the motion. However, you might need to check first if this is acceptable, if it risks the arm overshooting or oscillating around the endpoint. Designers need to think carefully about which tradeoffs they can make, and therefore what form their motion trajectories should take.

To make this simpler, there are standard trajectory profiles, such as the simple trapezoid, S-curve and contoured motion. Broadly speaking, these are progressively more refined, but also require more computational power to deliver.

To implement the chosen approach, many use the proportional-integral-derivative (PID) closed-loop control algorithm, which usually provides sufficiently accurate control of the motor and end effector.

Of course, when expanding into multiple axes and motors that need to be synchronised and coordinated closely, the magnitude of the control challenge increases.

A Standard or Custom Controller?

Motor controllers aren't usually the same as motor drivers, which control power to the motor. However, it is possible to integrate controllers with drivers and power devices for smaller motors.

If the motion required is relatively standard, there are fixed-function embedded-controller integrated circuits available. While these don't offer the flexibility of more complex controllers, some provide a choice of motion profiles and the ability to set key parameters. They're also relatively easy to use and low-cost.

> **A brushless DC motor or stepper motor is typically best in low- or moderate-power scenarios**

If the motion required is more sophisticated, or if the design demands additional connectivity, some form of user-programmable processor, using a field-programmable gate array (FPGA) or digital signal processor (DSP), is likely to be more appropriate. These provide much greater flexibility and a variety of auxiliary processing and support features.

There are many options available, some of which offer development kits, code packages and validation tools, helping robotics engineers harness the sophisticated capabilities they need to achieve with their control systems. ❖

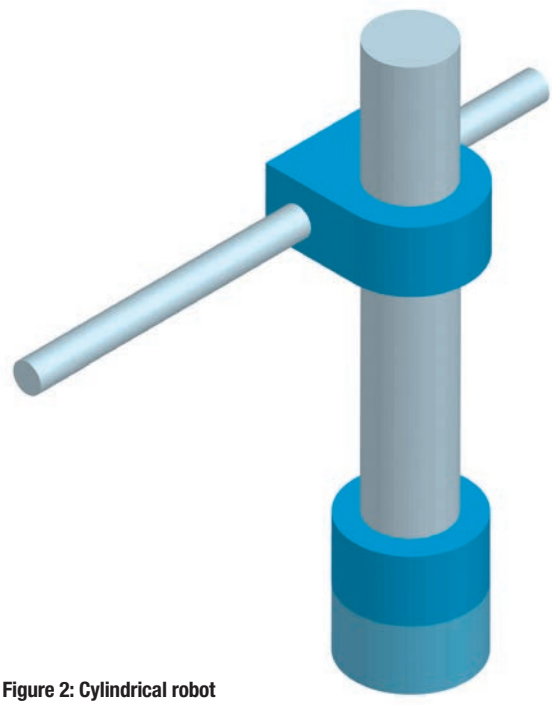

Figure 2: Cylindrical robot

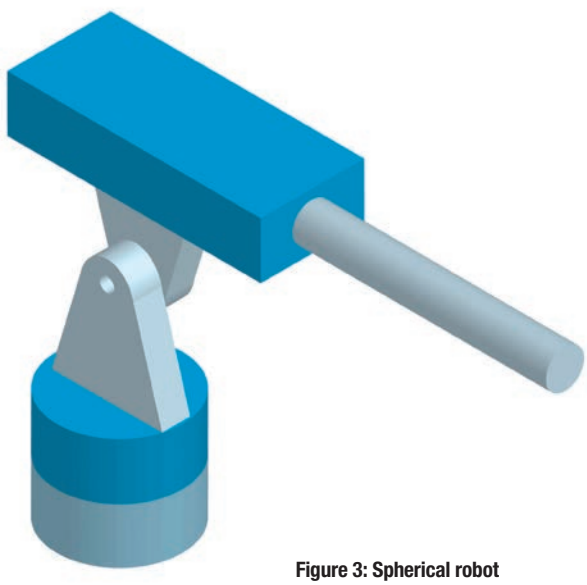

Figure 3: Spherical robot

Understanding instrumentation amplifiers – the secret of the 'diamond plot' tool

Instrumentation amplifiers are excellent for various measurements, including pressure and temperature. Their main tasks involve signal amplification and impedance adaptation.

In many cases, in-amps have a reference input pin. Adding a voltage at the reference pin will elevate the output signal by that voltage. This offers a simple and precise way to adjust the output of the instrumentation amplifier to the required input level of the ADC, creating the possibility for using the complete input span of the ADC with the benefit of higher resolution. An additional advantage is a very good common-mode rejection ratio (CMRR) and high precision in the case of a signal with a high common rail.

Figure 1 shows the internal schematic of an instrumentation amplifier in a typical three-opamp design.

If using an instrumentation amplifier, be aware that the maximum output voltage is dependent on the input signal (common-mode or differential), gain, power supply voltage and a possible limitation of the internal structure. In a three-opamp architecture, the first stage amplifier (inverting and non-inverting input) amplifies the input signal with a preset gain. The second stage works by subtraction; the output signal is built by subtraction of the two input signals. The reference voltage will be added to the signal, generating the combined output.

Based on this internal analogue signal generation, different factors could now lead to internal saturation and could reduce the maximum working area:

- Input voltage signal too high for the preset gain;
- Reference voltage too high for the generated output voltage signal;

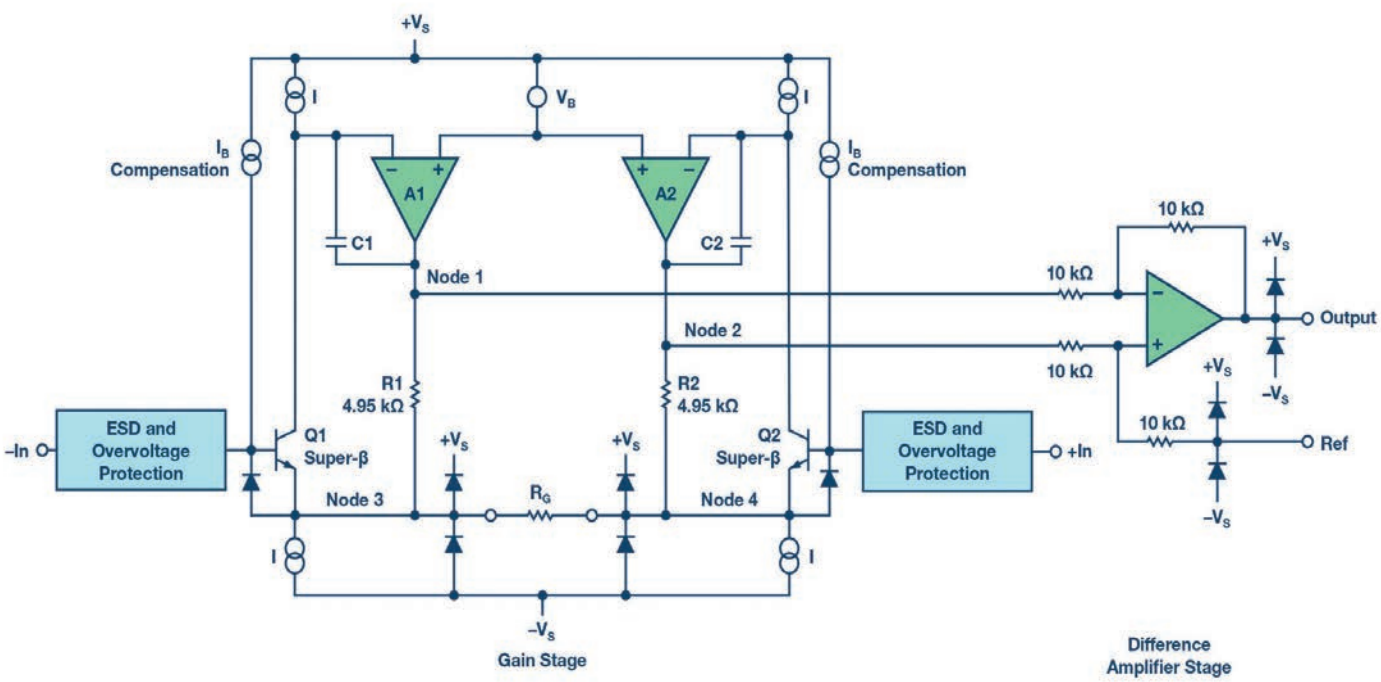

Figure 1: Internal architecture on a typical instrumentation amplifier

BY CHRISTOPH KÄMMERER, FIELD APPLICATION ENGINEER, ANALOG DEVICES

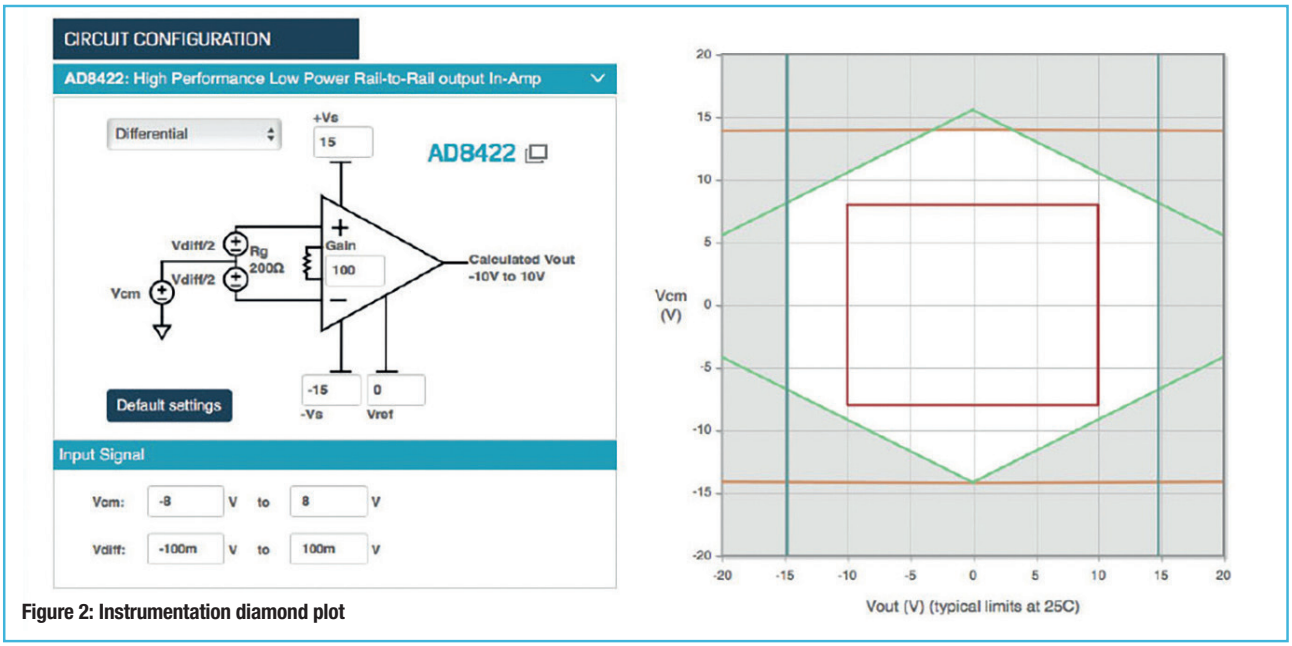

Figure 2: Instrumentation diamond plot

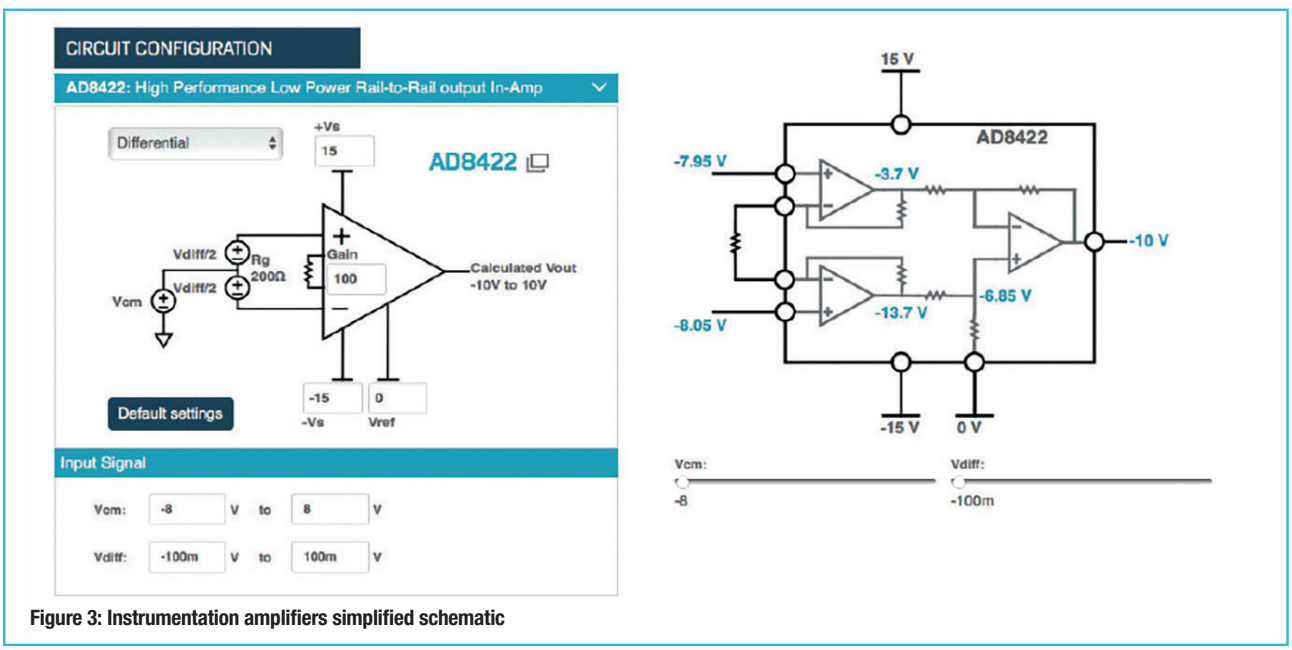

Figure 3: Instrumentation amplifiers simplified schematic

- The power supply voltage is too low.

Because the output voltage and instrumentation amplifier's working area depend on the maximum input signal, gain, reference voltage and limitations of the selected architecture, both are difficult to calculate. If you put these factors into a diagram, you would get a diamond-shaped graph, the so-called "diamond plot". The space of the graph represents the possible working area. The calculation is not easy, as there are multiple inputs and outputs.

Instrumentation Amplifier Diamond Plot Tool

The instrumentation amplifier diamond plot tool was developed by Analog Devices as an online means for such calculations. The tool automatically calculates possible configurations for the reference, input signal, supply voltage and gain for a required output signal. It graphically displays the possible parameter combinations for a particular output signal.

The tool contains the specifications for all Analog Devices instrumentation amplifiers, and it's fast and easy to use.

Figures 2-4 show the tool's graphical user interface and the windows for its diamond plot, internal circuity and recommended tool options.

Within the first window (Figure 2), you can enter all the required parameters, calculate the diamond plot and visualise it (possible parameters include input signal, gain, supply voltage and reference voltage). For the input signal, you can choose from a common-mode signal or a differential signal. In addition, the tool also helps determine the limitations of the selected amplifier and differentiate between input-output and internal restrictions. It is now possible to estimate the working area, too. In general, it is recommended not to operate very close to the plot limits.

The second window of the instrumentation amplifier diamond plot tool offers an internal view of the amplifier and displays a detailed schematic; see Figure 3. With this view, it is possible to see the technical details and the respective internal voltages, important when checking for possible errors in the design. A control mode is also offered to evaluate and rate the selected parameters and provide alternatives; see Figure 4. ❖

QUICK QUIZ

Access *www.analog.com/designtools/en/diamond/*, use a differential input for the AD8422, a gain of 100, a positive supply voltage of 15V, and a negative supply voltage of -15V; the reference voltage is 0. The common-mode voltage is 8V, and V_{DIFF} ranges from 100mV to 148.5mV. Assume that we are using the full temperature range and a load of 10kΩ. Using the diamond plot tool and data sheet, explain why this setup will not work.

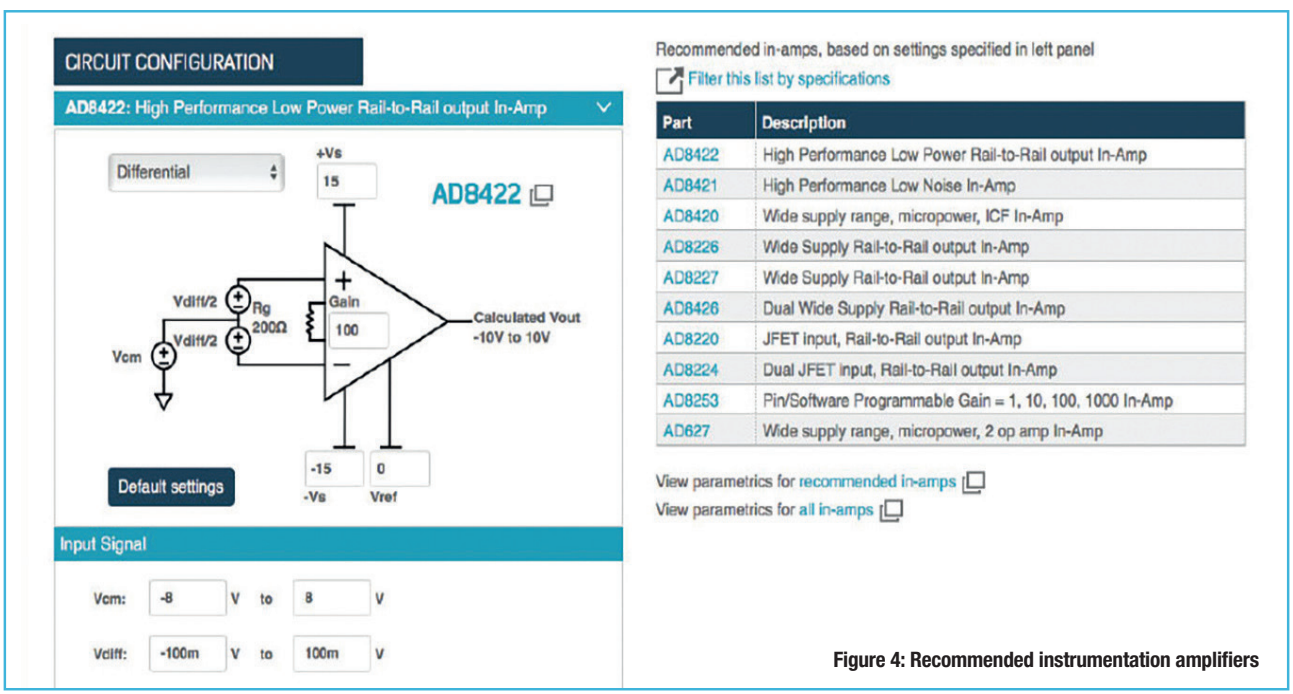

Figure 4: Recommended instrumentation amplifiers

Electronics WORLD

YOUR ESSENTIAL ELECTRONICS ENGINEERING MAGAZINE AND TECHNICAL HOW-TO-GUIDE

ELECTRONICS WORLD PROVIDES TECHNICAL FEATURES ON THE MOST IMPORTANT INDUSTRY AREAS, INCLUDING:

- RF
- Microwave
- Communications
- Nano measurement
- DSPs
- Digi
- Signal processing
- Lighting USB design
- Embedded
- Test and measurement
- Automotive
- Cables
- Connectors
- Power supplies
- Semiconductors
- Power supplies
- Robotics
- and much more...

A SUBSCRIPTION TO ELECTRONICS WORLD OFFERS:

- 12 monthly issues in digital format
- Regular topical supplements
- The Annual T&M Supplement
- Weekly email bulletin
- Comment and analysis from industry professionals
- Tips and tricks
- News and developments
- Product reviews
- Free invitations to our webinars

SUBSCRIBE TODAY FROM JUST £46 BY VISITING THE WEBSITE OR CALLING +44(0)1635 879 361

www.electronicsworld.co.uk/subscribe

Register for our free newsletter, please scan here

Ultra-wideband calibration-free 6-bit 4GSps folding-interpolating ADC

By Xiangmin Li and Zhuang Kang, Yangtze University College, and Liang Jia, University of Electronic Science and Technology, China

In high-speed optical communication receivers, high-speed analogue-to-digital converters (ADCs) provide sample information for use with DSP-based signal equalisation. High-speed ADCs are also needed for spectral identification of high-speed signals and can provide the interface to an on-chip Fast Fourier Transform (FFT) engine. But, to improve the performance of such systems, high sampling rate and medium-resolution ADCs are being pursued.

Ultra-Wideband ADCs

Ultra-wideband ADCs are required in a wide range of receiver applications, including digital radar receivers (DRRs) and ultra-wide bandwidth (UWB) communication. Figure 1 shows an example DDR system, where the antenna signal is directly digitised for further processing, after its conditioning. It can be employed in military surveillance, airborne early warning and target recognition. In these situations, low latency and no idle time for calibration are required of the ADC's analogue core. In some high-speed ADC designs with GHz sampling frequency, there's need for large latency because of the architecture's multiple pipeline stages. Dedicated time for calibration is necessary, since the CMOS technology's matching properties are poor.

In this architecture, the output of the track-and-hold circuit is applied to the input of four folding amplifiers, where it is compared to reference voltages generated by a resistor ladder

In addition to wide instantaneous bandwidth, accommodating high intermediate frequencies (IF) offers significant system advantages by reducing or eliminating costly RF down-conversion circuitry. Existing silicon-based designs with resolution higher than 6-bit and 1.33GSps sample rate use flash memory for high-speed operation. However, these designs do not successfully sustain their baseband effective number of bits (ENOB) performance at input frequencies higher than the sampling rate.

Here, we describe a calibration-free 6-bit 4GSps folding-interpolating monolithic ADC, fabricated in advanced SiGe BiCMOS technology. We use the folding-interpolating architecture because it consumes less power and occupies less space than its flash counterpart while sacrificing less speed and latency.

The matching properties of hetero-junction bipolar transistors (HBTs) are about ten times better than that of metal oxide semiconductor field effect transistors (MOSFETs). By using an on-chip highly-linear track-and-hold amplifier (THA), the architecture can sample input frequencies up to 5.5GHz with 5.45 ENOB performance, which is close to the ideal value of 6.

Block Diagram

The ADC's block diagram is shown in Figure 2. The folding-interpolating architecture exhibits flash-like speed of operation but requires fewer preamplifiers and comparators than the traditional flash approach. An equally important benefit of folding-interpolating is the significant reduction in capacitive loading on the analogue signal path, and the resultant contribution toward increased sampling rate.

In this architecture, the output of the track-and-hold circuit is applied to the input of four folding amplifiers, where it is compared to reference voltages generated by a resistor ladder. The output of the folding amplifiers is a set of phase-shifted sinusoid-like signals, which, in turn, are applied to an array of comparators. The outputs of the comparators are eventually converted to binary code by a digital encoder, to produce four least significant bits (LSBs). The two most significant bits (MSBs) are produced by a coarse quantiser.

To further reduce the die area and power dissipation, D_4 is extracted directly from comparator #16, and the coarse quantiser is only used to generate D_5. A bit-synchronisation circuit is included in the coarse quantiser to align the LSBs and MSBs.

The folding-interpolating architecture is highly applicable to high-resolution converters that need large analogue bandwidth. Figure 2 shows that each folding amplifier has five inputs, and each input consists of a pair of differential signals.

Circuit Design

An input THA improves the dynamic performance of an ADC. For gigahertz sampling rate operation, THA becomes essential to achieve the desired converter resolution with wide input bandwidth. By holding the analogue sample static during digitisation, the THA largely removes errors due to skews in the clock delivery of a large number of comparators, limited input bandwidth prior to latch regeneration, signal-dependent dynamic nonlinearity and aperture jitter.

As seen in Figure 3, The THA consists of an emitter-follower preamp driving a Schottky diode bridge, followed by an emitter-follower post-amplifier. The SiGe Schottky diodes used in this work provide

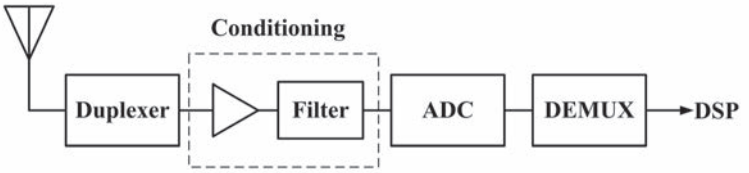

Figure 1: DRR system

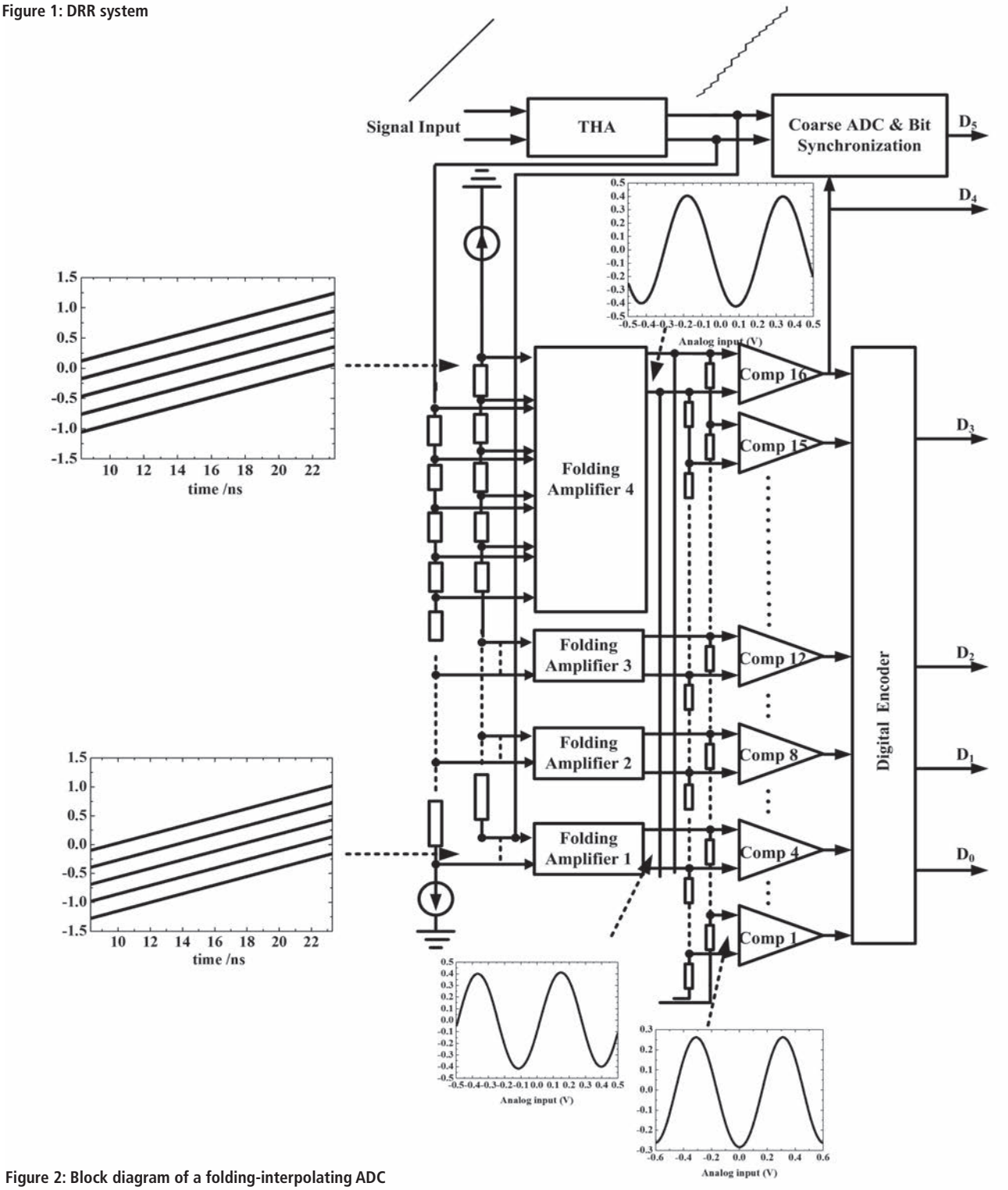

Figure 2: Block diagram of a folding-interpolating ADC

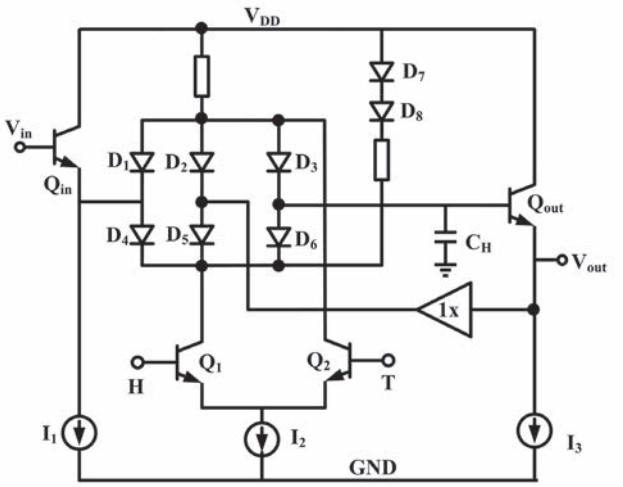

Figure 3: Simplified track-and-hold amplifier circuit

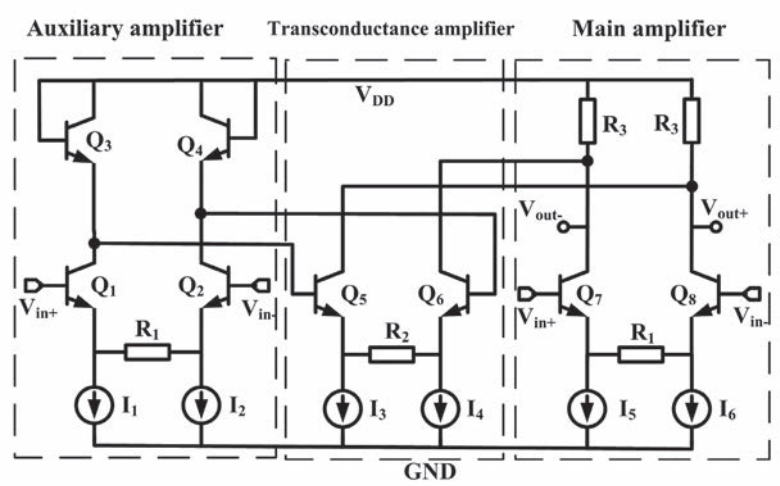

Figure 4: Highly linear input buffer

true majority-carrier device performance and are key to achieving sustained ADC performance at very high frequencies. The centre tap of the diode bridge is bootstrapped to reduce hold-pedestal distortion.

To achieve high resolution at the ADC output, we used a highly linear input buffer; see Figure 4. It consists of auxiliary, transconductance and main amplifiers. The auxiliary and main amplifiers together provide linearisation effect better than that of the traditional common emitter amplifier with resistor load and a wide input voltage swing.

The auxiliary amplifier loads consist of the Q_3 and Q_4 transistors that produce output voltages to drive the transconductance amplifier formed of Q_5, Q_6 and emitter resistor R_2. The transconductance amplifier is characterised by $G_m=1/R_2$ and is connected to the load resistor R_3 of the main amplifier.

In the input buffer, R_1 is set to be $2R_3$ for unity gain. Resistor R_2 is chosen to be lower than R_1 to cancel out the systematic gain error of the transconductance amplifier. As a result, the differential diode voltages are summed up with the main amplifier outputs at nodes V_{out+} and V_{out-}. Thus, distortion is compensated without requiring series connections of diodes and load resistors with the main amplifier's collector loads.

Folding Amplifiers

The basic function performed by folding amplifiers is the conversion of input signals into sinusoid-like output signals; see the topology of the folding amplifier used in our work in Figure 5.

Each folding amplifier with a folding factor of five generates four zero-crossings within the ADC's full-scale range (the one out-of-range folding factor minimises threshold distortion due to end effect). The folding amplifier is designed to be fully differential, which cancels any common-mode noise. Four folding amplifiers generate the required 16 zero-crossings.

Interpolation is implemented using 4× resistive-string networks because of their simplicity and power efficiency, and, also, because using resistor averaging improves the ADC's linearity. In the folding architecture, the number of folding amplifiers is equal to the number of reference levels in the fine quantiser. However, this problem can be solved by creating only a small number of folding signals and deriving the other folding signals by resistive interpolation between the outputs of two adjacent signals.

The circuit diagram for interpolation between two folding amplifier outputs is shown in Figure 6. Here, the folding signals of V_1, V_2 and V_3 can be obtained directly from V_0 and V_4, which are the outputs of two consecutive folding amplifiers.

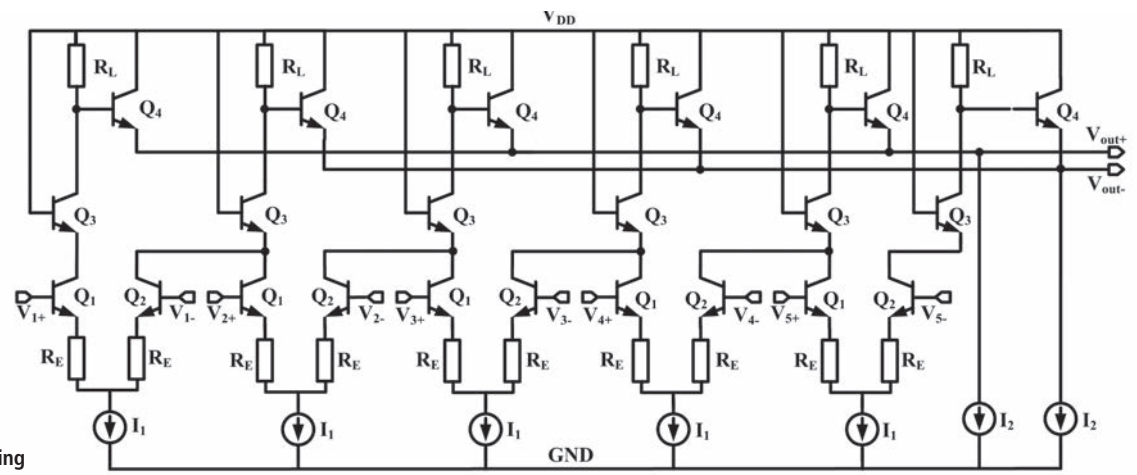

Figure 5: Folding amplifier

$$V_1 = 3V_0/4 + V_4/4 \quad (1a)$$

$$V_2 = V_0/2 + V_4/2 \quad (1b)$$

$$V_3 = V_0/4 + 3V_4/4 \quad (1c)$$

The transfer function of the folding-interpolating circuits is shown in Figure 7. Observe that 64 thresholds are within the analogue input full-scale range to provide the overall 6-bit resolution. In the figure, curves 1, 2, 3 and 4 represent the output signals of the folding amplifiers 1, 2, 3 and 4, respectively.

Complete Comparator Circuit

The complete comparator circuit used in our work is shown in Figure 8. It consists of a preamplifier and two cascaded differential comparators in a master-slave configuration. The preamplifier is designed in a differential amplifier configuration to achieve the required gain and bandwidth.

The master-slave comparators are identical and driven by complementary clocks. When the master comparator goes into track mode, the slave comparator is in latch mode and holds its digital value. Alternatively, when the master comparator goes into latch mode, the slave comparator is in track mode and tracks the latched signal of the master comparator. This ensures that a fully digital output is obtained at the output of the comparator. Buffers (emitter followers Q_3) are used to level shift the signals between the master and slave comparators and the preamplifier.

Digital Encoder and Coarse Quantiser

In the fine quantiser, the four LSBs (D_0-D_3) are extracted using a digital encoder. The encoder consists of three functional blocks: an XOR array, a bubble error correction (BEC) circuit, and a 15-to-4 ROM. A set of circular codes generated by the comparators are applied to the XOR array where they are converted into a set of 1-of-N codes. The 1-of-N codes are then sent to the BEC block where any error inside the circular codes is corrected by virtue of the NOR logical operation. The output of the BEC block is applied to the 15-to-4 ROM, where the final binary codes of the ADC are generated. The MSB D_4 is extracted directly from comparator #16 and the remaining one MSB D_5 is obtained by the coarse quantiser.

Implementation and Results

For test purpose, a 1:4 demultiplexer (DEMUX) with output drivers has been implemented on-chip. The ADC-DEMUX chain has been fabricated in HHNEC 0.18µm SiGe BiCMOS technology. The ADC occupies an area of 3.8mm×2.92mm; see Figure 9.

Two power supplies used for the analogue building blocks (AVCC = 3V) and the digital parts (DVCC = 3V). Of the 212 bonding pads, 120 are dedicated to the power and ground networks, to supply enough current with low bond-wire inductance.

We performed an ADC test using a high-speed evaluation board;

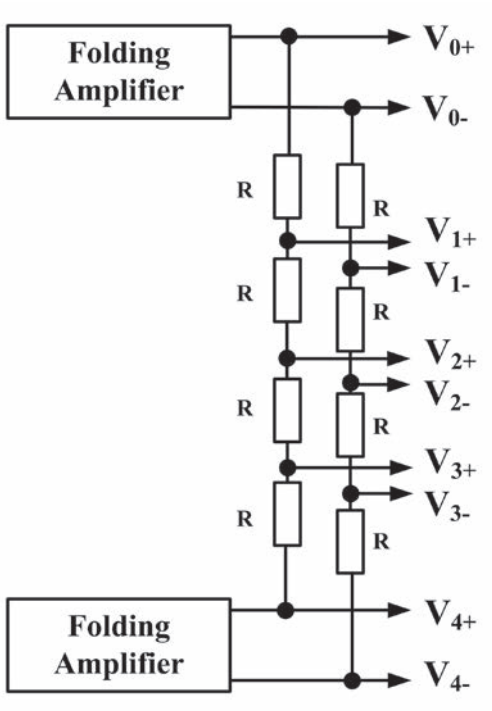

Figure 6: Interpolation between two folding amplifier outputs

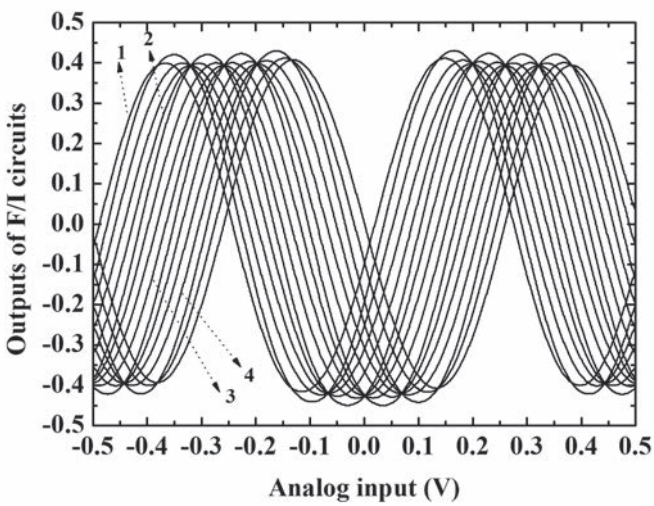

Figure 7: Transfer function of the folding-interpolating circuits

see the setup in Figure 10. Two wide-bandwidth baluns convert the outputs of the signal generators to supply the ADC with a differential analogue input and a differential clock input, respectively. The output data was captured with a high-speed data acquisition unit for analysis. At the clock frequency of 4GHz, the ADC's power dissipation is 1.1W.

Figure 11 shows the measured static linearity of DNL and integral nonlinearity (INL) at 4GSps, where the peak DNL is 0.35 LSB and the peak INL is 0.55 LSB, respectively. The high DNL and INL result from the interpolation topology, the nonlinearities in the sampling circuit and the resistive reference ladder.

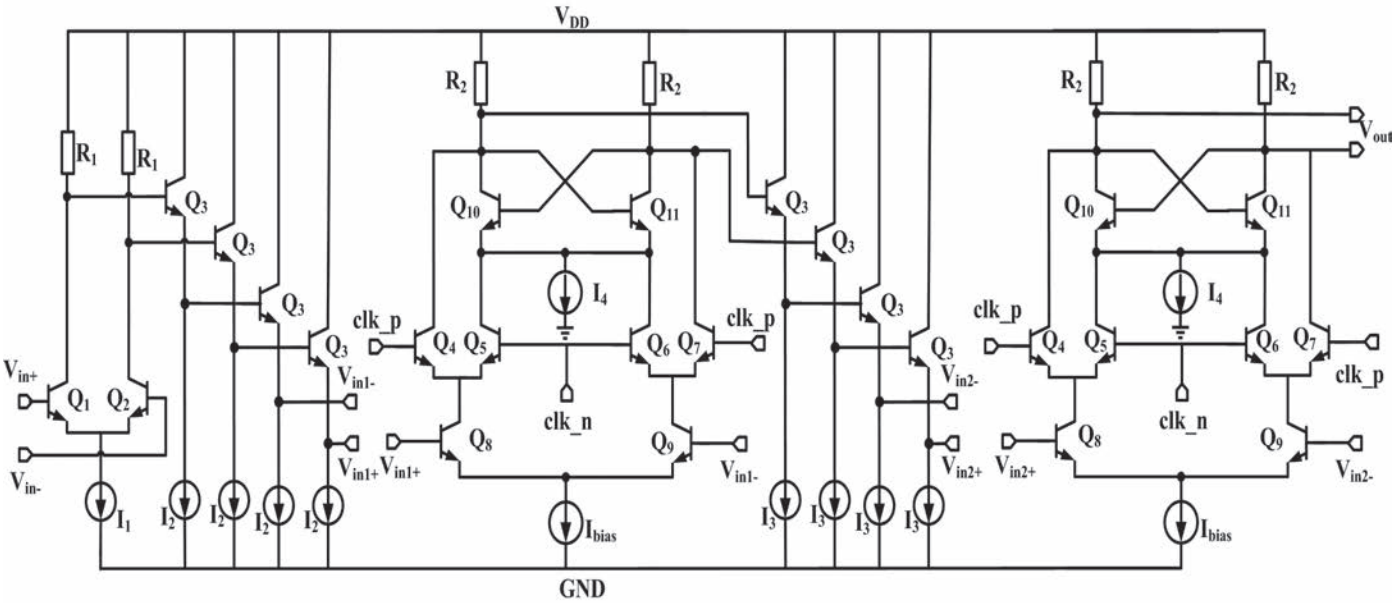

Figure 8: Master-slave comparator

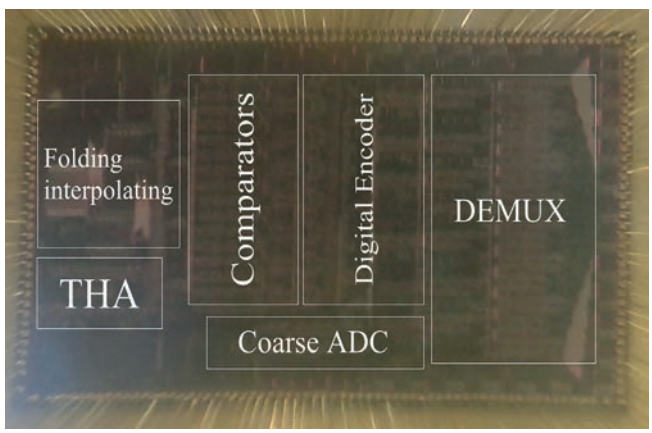

Figure 9: Chip microphotograph of the ADC-DEMUX chain

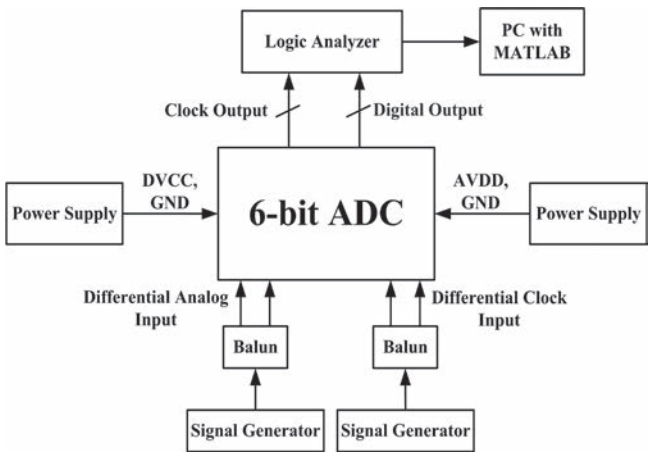

Figure 10: Block diagram of the ADC test setup

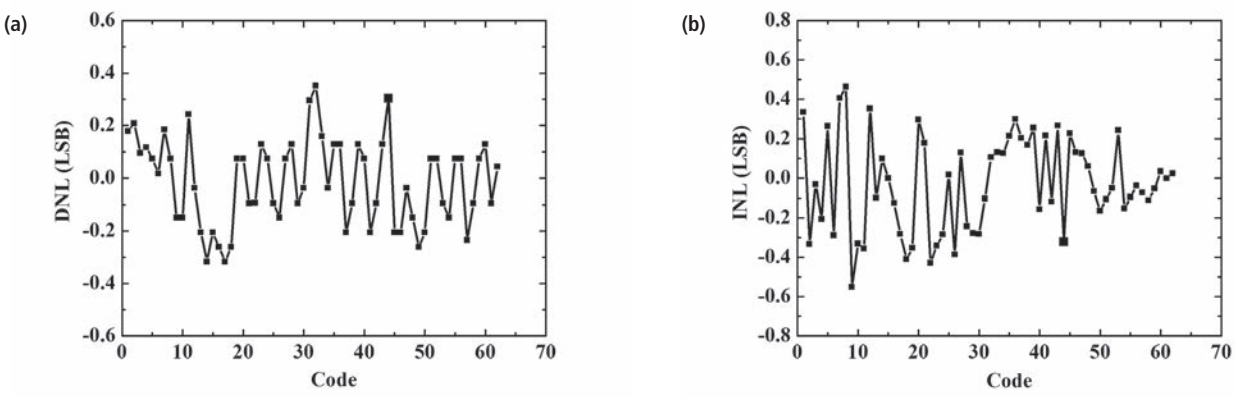

Figure 11: Measured (a) DNL; and (b) INL, at 4GSps

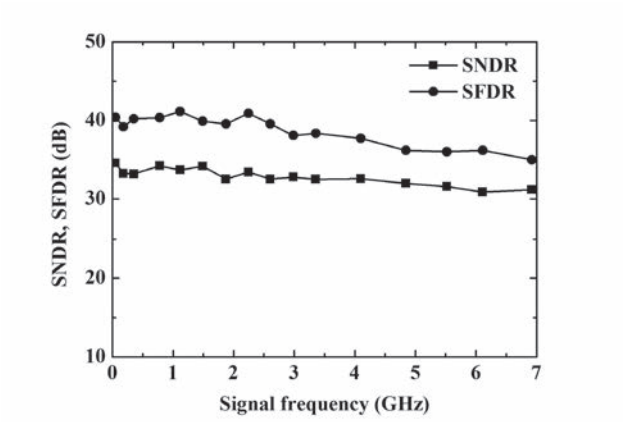

Figure 12: Measured SNDR and SFDR at 4GSps

To measure the ADC's dynamic performance, a low distortion sinewave input was applied to it, and the reconstructed waveform was obtained by binary weighted adding of the ADC's output codes. The reconstructed waveform was then analysed using MATLAB, to calculate the signal-to-noise-and-distortion ratio (SNDR), ENOB and spur-free dynamic range (SFDR). Figure 12 shows the ADC's SNDR and SFDR at different input frequencies when the converter is clocked at a sampling frequency of 4GSps.

PARAMETER	VALUE
Technology	0.18µm SiGe BiCMOS
Sampling rate	4GSps
Resolution	6 bits
Input range	$1V_{p-p}$
Maximum DNL	0.35 LSB
Maximum INL	0.55 LSB
SNDR	34.57dB
Peak ENOB	5.45
SFDR	40.4dB
ERBW	5.5GHz
Power dissipation	1.1W
Chip area	3.8mm × 2.92mm

Table 1: Summary of the 6-bit ADC characteristics

At low frequencies, the converter's SNDR is 34.57dB (5.45 ENOB). The ERBW where the SNDR drops 3dB from its low frequency value is 5.5GHz.

Table 1 summarises the 6-bit ADC's main characteristics. ❖

Structural design of a space active phased-array antenna

Congsi Wang, Haihua Li and Kang Ying, Xidian University, Meng Wang, Research Institute of the Shaanxi Huanghe Group, Zhihai Wang, CETC Research Institute, Xuelin Peng, Nanjing Research Institute of Electronics Technology, and Shaoxi Wang, Northwestern Polytechnical University, China

More and more is being required of space antennas: multi-functionality, multi-band coverage, long range, higher transmitting power, yet lower power consumption, driven by the need for ever-increasing data-transfer capacities. Earlier antennas had small apertures and low gain, making them unsuitable for these growing requirements. Space-deployable reflector antennas solved some of the problems, but their reliance on mechanical scanning causes inertia and low speed. Heavily relying on mechanical components also leads to problems such as reduced reliability and increased weight.

Active phased-array antennas based on satellite platforms offer large apertures and are light. Their high gain, long range, rapid beam scanning, agile beam steering and multi-beam forming satisfy the needs of spaceborne equipment.

Space Active Phased-Array Antennas Structures

Currently, there are two main types of spaceborne, deployable phased-array antennas: folded planar and flexible.

A honeycomb 'sandwich' structure made of composite material is widely used in these antennas, since it is light and strong, with good bending performance, high temperature resistance, high surface precision, a simple forming process, and more (Figure 1). Unfortunately, the larger the aperture, the heavier the antenna.

The thin-film flexible array antenna is also light and small, easy to fold and unfold, and very reliable. Its main feature is that its high-frequency receive/transmit equipment is inside it, with the high-frequency feeder on its back, making the overall system flexible and easy to fold. This approach makes the space active phased-array antenna system three times lighter.

Figures 2 and 3 show flexible deployable array antennas with two modes: folded or crimp contraction during launch, and deployed through inflatable or line expansion after entering orbit.

Figure 4 shows an inflatable thin-film array antenna with aperture of 3m x 100m. This type can operate at very high frequencies. For still larger apertures and even better surface accuracy, an expanded form of antenna consisting of a combination of rigid and flexible panels is currently a hot research topic; see Figure 5.

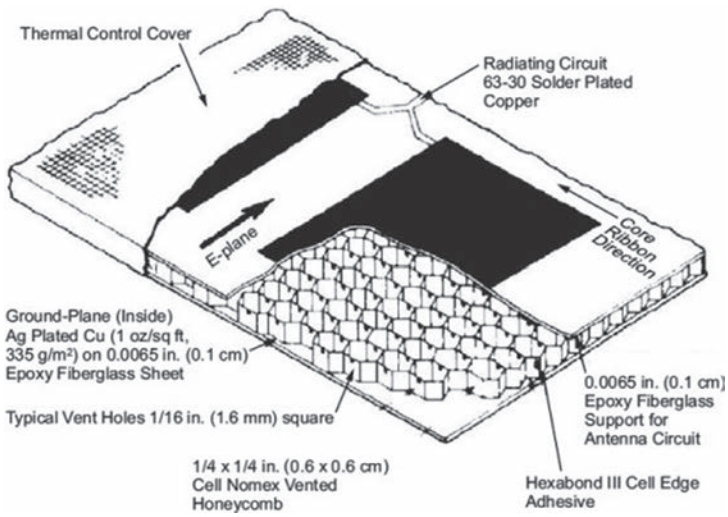

Figure 1: Aluminum honeycomb panel of the SEASAT-1 satellite

Parameters Affecting Antenna Performance

In the space active phased-array antenna, there is interaction between several parameters: structural displacement, electromagnetic performance and temperature:

1. Change in antenna structure (such as the deployable mechanism) and environmental loads (for example, Sun exposure and the shadow zone) can affect the structural displacement field.
2. Change in the displacement field changes the electromagnetic field. For instance, an attitude change of the satellite can bend the array structure, changing the position of the array excitation source.
3. Change in the temperature field influences transmission performance, which then impacts the electromagnetic field; for example, the accuracy of the phase shifter is very sensitive to junction temperature.
4. Change in the temperature field also impacts the structural displacement field; for example, inconsistent temperature of the antenna structure produces thermal stress, leading to structure deformation or flutter.

All of these factors will have inevitable consequences on the electrical performance of the space active phased-array antenna.

PARAMETERS	ALOS	ALOS-2
High-power amplifier	Si bipolar transistors	Gallium-nitride transistors
Power (W)	25	34
Operation bandwidth (MHz)	28	85
Number of T/R components	80	180
Efficiency (%)	25	35
Noise coefficient (dB)	2.9	2.9
Size of T/R components (mm)	203 x 117 x 23.5	200 x 110 x 14.6
T/R components weight (g)	675	400

Table 1: Parameter comparison of T/R modules in two kinds of satellite antennas

Essential Components

Successful development of a spaceborne deployable active phased-array antenna system involves seven key subsystems: T/R modules, phase shifter, feed system, radiating element, power supply, deployable mechanism and thermal control. In contrast to the ground phased-array antenna, a spaceborne version has much tighter requirements in terms of electrical performance, including beam shape and efficiency. As for selection of the material, it's crucial to use a light sheet material, to ensure the antenna has a large aperture and extensibility, and is lightweight.

When choosing the electronic components, small size and lightweight are also key. The antenna needs to withstand the long-term effects of infrared radiation and high temperature from the Sun. Here, the temperature environment is quite demanding, so thermal design of the system is extremely important.

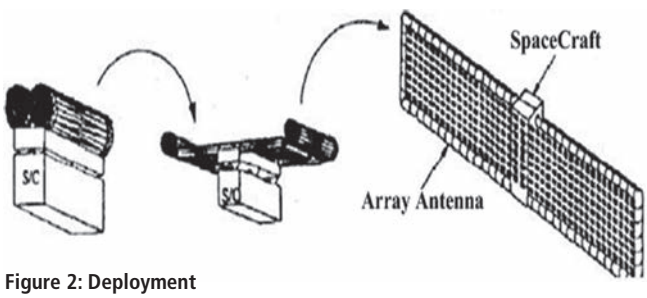

Figure 2: Deployment stages of phased-array antenna using inflatable expansion

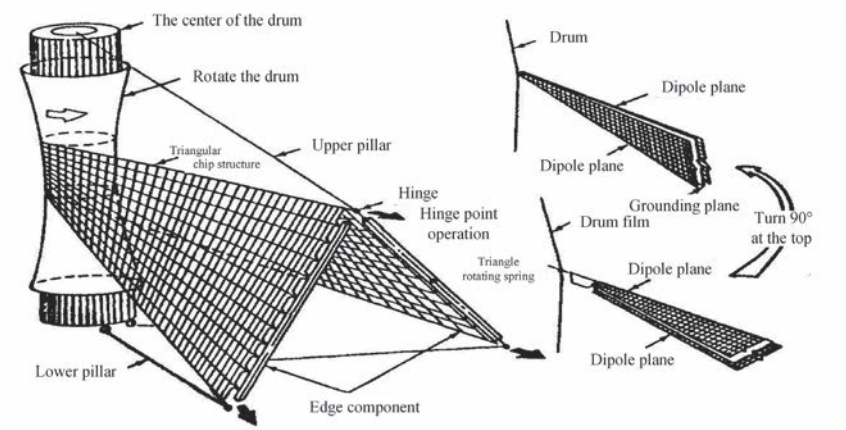

Figure 3: Deployment of phased-array antenna using line expansion

T/R module

There are quite a few T/R (transmitter/receiver) modules in this type antenna, and their weight, size, efficiency, bandwidth and noise figure are important to the final design of the system; see Table 1.

With the rapid development of monolithic microwave integrated circuit (MMIC) technology, the weight and size of T/R modules will be significantly reduced; see Figure 6.

Phase shifter

The space deployable active phased-array antenna consists of many antenna elements, and each unit (or sub-array, also comprising several elements) can do beam scanning by changing the phase of its phase shifter. This is done electronically, affecting the beam shape and speed of its scanning. The number of beams and their movement can be set in advance.

The electronically-controlled phase shifter is an essential component of this type antenna, and its main requirements are: high accuracy in phase shifting; stable phase-shifting value that doesn't change with temperature or signal level; low insertion loss and VSWR; high power capacity (for the transmitting array); quick phase shifting; and low power consumption. And, of course, small size, light weight, long life and low cost are just as important.

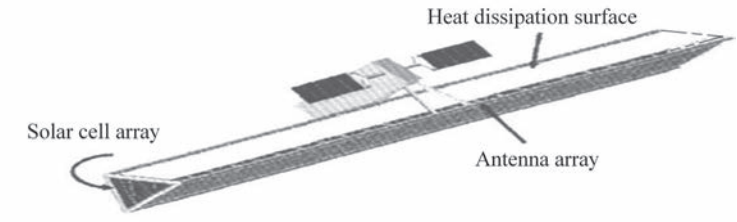

Figure 4: Inflatable thin-film array antenna with 3m x 100m aperture

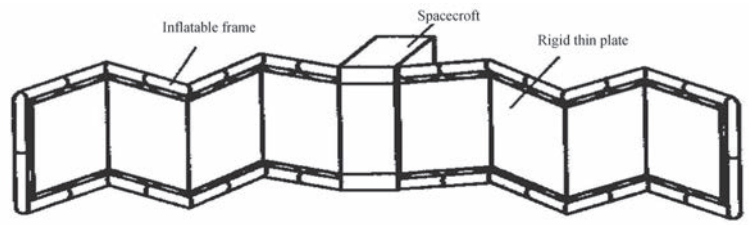

Figure 5: Expanded form of rigid-flexible combination

In the field of space T/R modules, RF MEMS devices are a promising technology, because they enable smaller and lighter phased-array antennas. They require little power, so they lessen the design load since they don't need cooling, extending the antenna's operational life. Compared to traditional T/R components, insertion loss of MEMS T/R components is much lower, thus it takes half or even a quarter of the T/R in the system to meet the functional requirements of the antenna. Due to MEMS devices' high linearity, isolation and wide bandwidth, using MEMS T/R in the antenna expands its bandwidth and sensitivity and reduces steering errors.

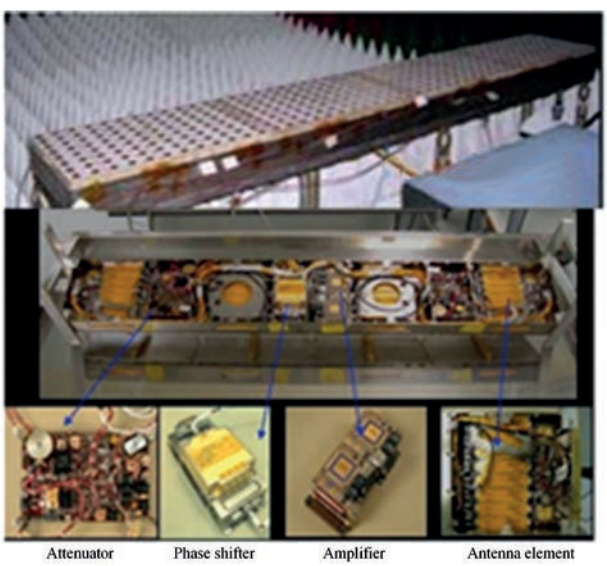

Figure 6: Applications of MMIC technology

Feed system

In an active phased-array antenna, each unit's signal is sent to the receiver, commonly known as "feed". The phase distribution for all antenna element channels determines the beam shape and scan, known as "phase feeding".

In the SEASAT-1 satellite, antenna elements are connected using a microstrip transmission line; the antenna is fed by a coaxial line. Due to the large number of elements, the feed network becomes complex, making the layout of the feed system critical in meeting the antenna's electrical requirements; see Figure 7.

Since amplitude and phase characteristics of T/R components are temperature-sensitive, it is particularly important to control the temperature distribution of all T/R modules on the array surface. In the feed system, special environmental control measures are used for the T/R modules, in which the amplitude and phase performance of each module are strictly controlled. Of course, strict quality control is also necessary for all components during their production.

Radiating element

Although the radiating element, phase shifter and feed network are the three basic parts of the active phased-array antenna, its performance is tightly linked to the radiating element. At present, there are two main types of space deployable phased-array elements: microstrip and waveguide slotted antenna.

Table 2 shows the advantages of microstrip antennas; they are low in profile, light, small, simple in structure, low in cost and can be integrated with the feed network in coplanar configuration. On the negative side, they are low in efficiency (below 50%) and their bandwidth is relatively narrow at the typical C-band operating frequency.

The efficiency of the waveguide slotted antenna is up to 70%, and it offers high isolation and low profile. But, this type antenna has a complex structure and a difficult manufacturing process. It is mostly used for frequencies above the C band.

A key goal to successful antenna element design is to meet the electrical and structural requirements simultaneously, including size, weight, reliability and ease of installation.

Power supply

For any satellite platform, its power supply's size and weight limits are extremely strict. Therefore, the array's power supply, with high power density, high reliability and high efficiency is one of the key components of the space active phased-array antenna.

Using high-efficiency and high-density packaging power (HDPP) can decrease the size and weight of the entire antenna array; however, the high-power phased-array antennas often need several hundred amperes of current, which imposes great risks on the space application. At present, the usual approach

Parameters	Microstrip antenna	Waveguide slotted antenna
Bandwidth	Narrow	Wide
Gain	Low	High
Efficiency	Low	High
Environmental suitability	Bad	Better
Processing technology	Low-cost lithography	High-precision numerical control
Cost	Low	Higher

Table 2: Comparisons between microstrip and waveguide slotted antennas

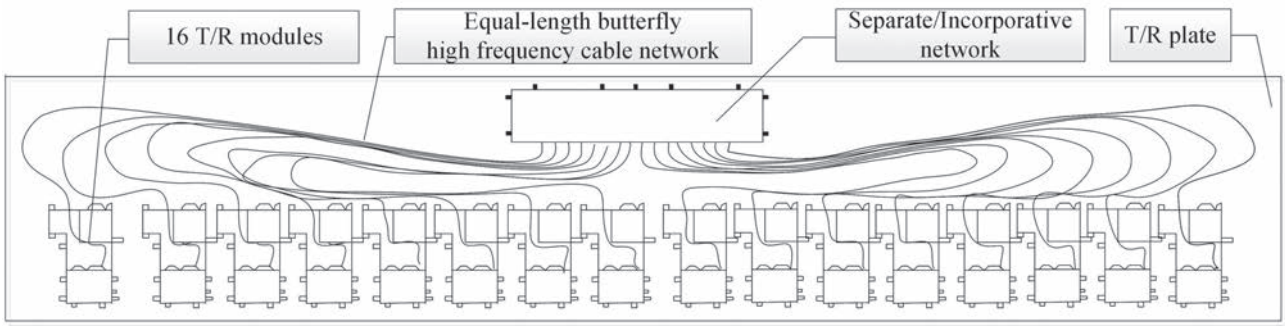

Figure 7: Example layout of a space active feed system

is to use many distributed current modules, each supplying a part of the subarray so the large current can be divided into smaller currents. This approach also makes it easy to realise redundant backup, improving the reliability of the antenna.

Figure 8 shows the high-density packaging of a large lithium-ion battery, comprising 2016 lithium-ion units (9S-224P configuration: nine cells in series and 224 in a series-parallel topology), which can support the 17.8kW peak power required by the space antenna. The power supply is 136kg, with a minimum life of five years and reliability up to 99.9%.

The battery is made of eight identical modules, each with two parallel electric connectors and two power buses connected to current sensors. This kind of high-density packaging can meet the high power requirements of the active phased-array antenna by changing the configuration and number of modules, making the system more flexible and with lower development costs.

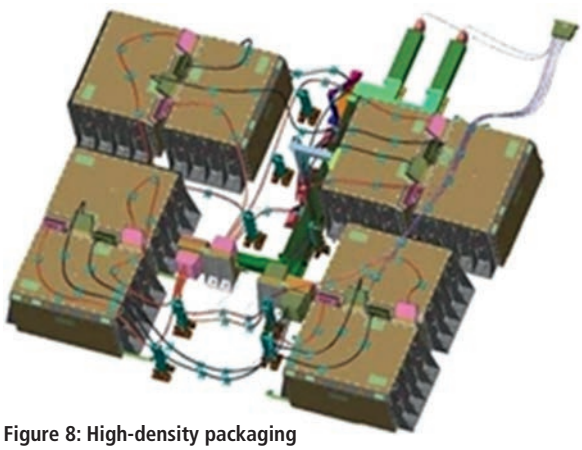

Figure 8: High-density packaging of a large lithium-ion battery

Deployable mechanism

The deployable mechanism of a spaceborne active phased-array antenna can take three forms: folding-deploying structure (Figure 9), single-reel rolling structure (Figure 10) and double-reel rolling structure (Figure 11). The complex folding-deployable mechanism is first choice for the antenna system's normal operation, so its reliability must be guaranteed.

Thermal control

A satellite antenna is subject to many environmental challenges, including during its launch, orbit injection,

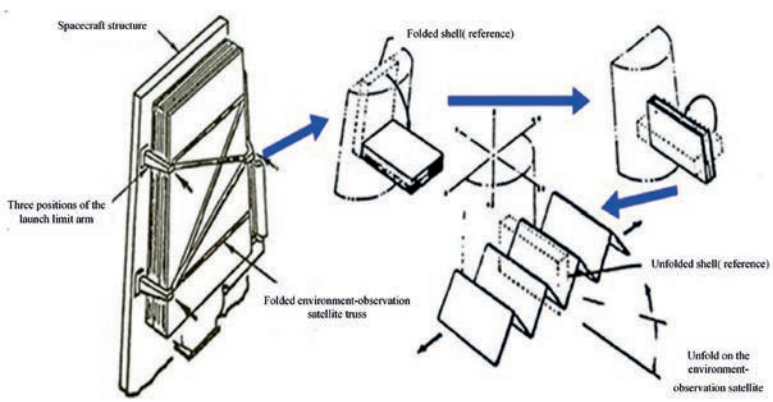

Figure 9: Folding-deploying structure

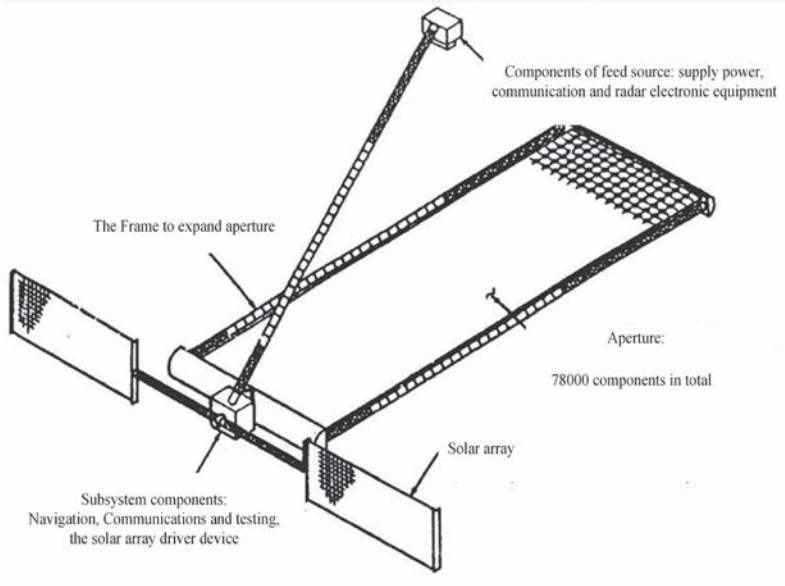

Figure 10: Single-reel rolling structure

operation and ground return. Especially in orbit or during space travel, the Earth's atmosphere no longer protects the spacecraft, which is subjected to effects including vacuum, cold black, solar radiation, weak magnetic field, particle radiation, magnetospheric substorm, microgravity, atomic oxygen, ionospheric plasma, and more. Out of these, heat is one of the most important environmental factors, since the spacecraft needs to endure long stretches of infrared radiation and also serve as a low-temperature heat-sink for solar radiation. Additionally, there are periodic, severe temperature field changes, with fluctuations up to ±200°C.

Microgravity and high vacuum make heat transfer even more difficult, resulting in large difference between the heat transfer process in space and that on the ground. A large temperature gradient produces many adverse effects on the satellite: on the one hand, larger thermal stress can affect the position of the elements, thereby affecting the antenna's electrical performance; and on the other, if the temperature of the satellite component is too high, it will affect normal device performance, or even cause component failure.

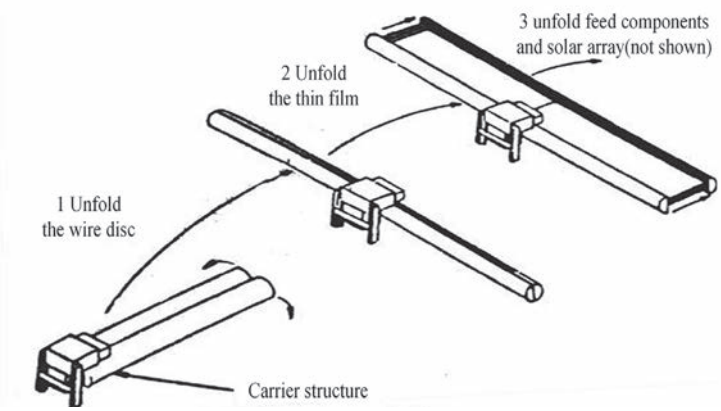

Figure 11: Double-reel rolling structure

MEMS Technology

The development of MEMS technology provides a new way to solve problems such as high heat flux density and small heat dissipation in satellite antenna systems. One objective is to develop an ultra-low-cost and low-power light phased-array antenna using MEMS thermal control technology and MEMS phase shifters. The whole thermal control system can be integrated on a single circuit board through MEMS processing technology. In contrast to traditional electromechanical systems, MEMS technology makes such integration much tighter, multi-functional, smart and reliable.

Development Trends

With increased use of space communications, electronic surveillance, navigation and environmental monitoring, there's a greater demand for spaceborne active phased-array antenna. In the future we'll see even further development of deployable active phased-array antennas, including:

(1) A study of electromechanical coupling in space antennas. Mechanical, electromagnetic and thermal coupling problems exist widely in high-performance electronic equipment. In spaceborne active-phased array antennas, structural displacement, electromagnetic and temperature fields interact, affecting its electrical performance.

(2) Focus on breaking through the limitations imposed on the antenna by the severe space environment. The main obstacle is adaptability of the active phased-array antenna to the space environment, where thermal control is crucial; this influences the choice of materials, technologies, control programs and other aspects of these type antennas.

(3) As the working frequency of the active phased-array antenna increases, there's need for larger apertures, greater extensibility, lighter weight, and higher reliability and integration. This involves the design and manufacture of high-performance T/R modules, feed networks, radiating elements, power supplies and antenna deployable mechanisms on thin plates or thin-film materials. Advanced composite materials, MMIC and RF MEMS devices can greatly reduce the volume and mass of the phased-array system.

For antenna and aerospace engineers, although the history of the spaceborne deployable active-phased array antenna is long and complex, this ongoing research remains very important. ❖

Scanning acoustic microscopy, from lab to high-throughput fab

By Jeff Elliott, technical writer based in the US

The growing volumes of silicon ingots, wafers, integrated circuits (ICs), MEMS and other electronic packages requires equipment that performs non-destructive imaging and materials analysis. In addition, the continuously evolving high-volume production processes are rapidly migrating beyond industry standards. New device designs, packaging methods, shrinking dimensions, bonded wafer interfaces and increased production yields are driving a market for improved production equipment. Challenges include higher levels of automation integration for component handling, improved cleanroom performance requirements, and scanning of ever-smaller components and interface connections. These conditions all advance scanning acoustic microscopy (SAM) technology, rapidly establishing it as a method of choice.

SAM Technology

SAM uses ultrasound waves to non-destructively examine internal structures, interfaces and surfaces of opaque substrates. It works by directing focused sound from a transducer at a small point on a target object. The sound hitting the object is either scattered, absorbed, reflected (scattered at 180°) or transmitted (scattered at 0°). By detecting the direction of scattered pulses and the 'time of flight', the presence of a boundary or object can be determined along with its distance.

A unique characteristic of acoustic microscopy is its ability to image the interaction of acoustic waves with the elastic properties of a specimen, allowing imaging the interior of an opaque material. To produce an image, samples are scanned point by point and line by line. Scanning modes range from single-layer views to tray scans and cross-sections. Multi-layer scans can include up to 50 independent layers. The resulting acoustic signatures can be put together into three-dimensional images that are analysed to detect and characterise device flaws such as cracks, delamination, inclusions and voids in bonding interfaces, and to evaluate soldering and other interface connections.

"Using ultrasound provides a clear advantage in ensuring good adhesion and mechanical integrity of devices," said Peter Hoffrogge, Product Manager of PVA TePla Analytical Systems, a company that designs and manufactures advanced scanning acoustic microscopes. Compared to alternative techniques like X-ray, used to evaluate volumes and densities, ultrasound looks at interfaces, says Hoffrogge. "In an example of a sintered connection on a power device, the gaps are only a few nanometers," he said. "With X-ray there's no contrast, so you can't tell whether the die has adhesion through the interlay or not. With ultrasound, it is easy to see."

The challenge today is to perform this inspection at extremely high throughput with 100% accuracy in identifying and removing components that don't meet the quality requirements. Often, these defects can occur in different layers of the device, calling for advanced equipment that can simultaneously inspect several layers and scanning multiple samples in handling trays in an automated way to accelerate the process.

Transducers can be adapted to each application or specific customer device and inspection requirement, ensuring the highest level of defect detection

However, as with other inspection systems, increased throughput requirements traditionally have required sacrificing image resolution. Fortunately, said Hoffrogge, today's advanced inspection equipment can overcome these limitations. Much of it is custom designed to be integrated into other high-volume manufacturing systems, such as those inspecting crystal ingots, wafers and electronics packages in a range of standard sizes. For items with more unique product geometries or sizes, equipment can be semi-customised to meet the requirements of an application based on established, common components.

Pre-Developed, Integrated Systems

Today, SAM equipment exists that specifically handles standardised items such as bonded wafer inspection of MEMS, CMOS imaging sensors, and others. The equipment tests for inclusions or delaminated areas in the bonding interfaces and other defects.

"Typically, damage inspection is performed in a late stage of production to make sure the device is error-free, 100% flawless. This is typically done before dicing," says Hoffrogge.

A bonded wafer inspection tool can be optimised for high

throughput with four transducers and automated wafer handling. Cassette-loading systems are quick (open load port, SMIF, FOUP or customised input and output cassettes) for robots handling 5-12inch wafers and integrated scanners for wafer tracking, along with other features required of such systems.

For volume inspection of single-crystal ingots (e.g. Si, Ge, GaAs) a multiple-transducer scanning system (four heads) is used to estimate the 3D location of defects inside the crystal, so the tool can analyse voids and inclusions, estimating their depth and size. The tool can inspect 5-12inch Si ingots up to 400mm thickness and 75kg weight. Defect resolution may approach 100µm voids in silicon.

Hoffrogge says there are many systems in production, performing inline inspection of sensitive electronic devices transported in JEDEC trays. Regardless of the type of component inspected, each system includes integrated data analysis and automation software, GEM/SECS interface for fab-host communication and other key features.

Specific Equipment

When even higher throughput is required, multiple transducers can be used on a single substrate, with the images then stitched together, or multiple transducers can simultaneously scan multiple substrates.

Throughput can also be increased by incorporating ultra-fast single- or dual-gantry scanning systems or 6-axis robots. Other possible add-ons include axis-rotation (flipping), vacuum chucks and customised water tanks.

Hoffrogge suggests working with a company with a large portfolio of core, standard components to use or modify for a rapid and specific inspection solution. Having the complete value chain available from one vendor can speed the development process from the start through to complete process qualification, providing maximum value.

Even transducers, at the heart of all SAM systems, can be custom-manufactured to meet specific scanning requirements. Transducers can be adapted to each application or specific customer device and inspection requirement, ensuring the highest level of defect detection.

Some companies design and manufacture transducers in a very wide frequency range, from 3-2000MHz. They perform this work in-house, utilising proprietary thin-film technology developed over many years.

"It is possible to manufacture transducers within the standard cost and lead times of the industry," said Hoffrogge. "Having all the equipment for manufacturing and testing in-house, eliminates the need to rely on third parties for items such as optical components, where there are often very significant lead times." ❖

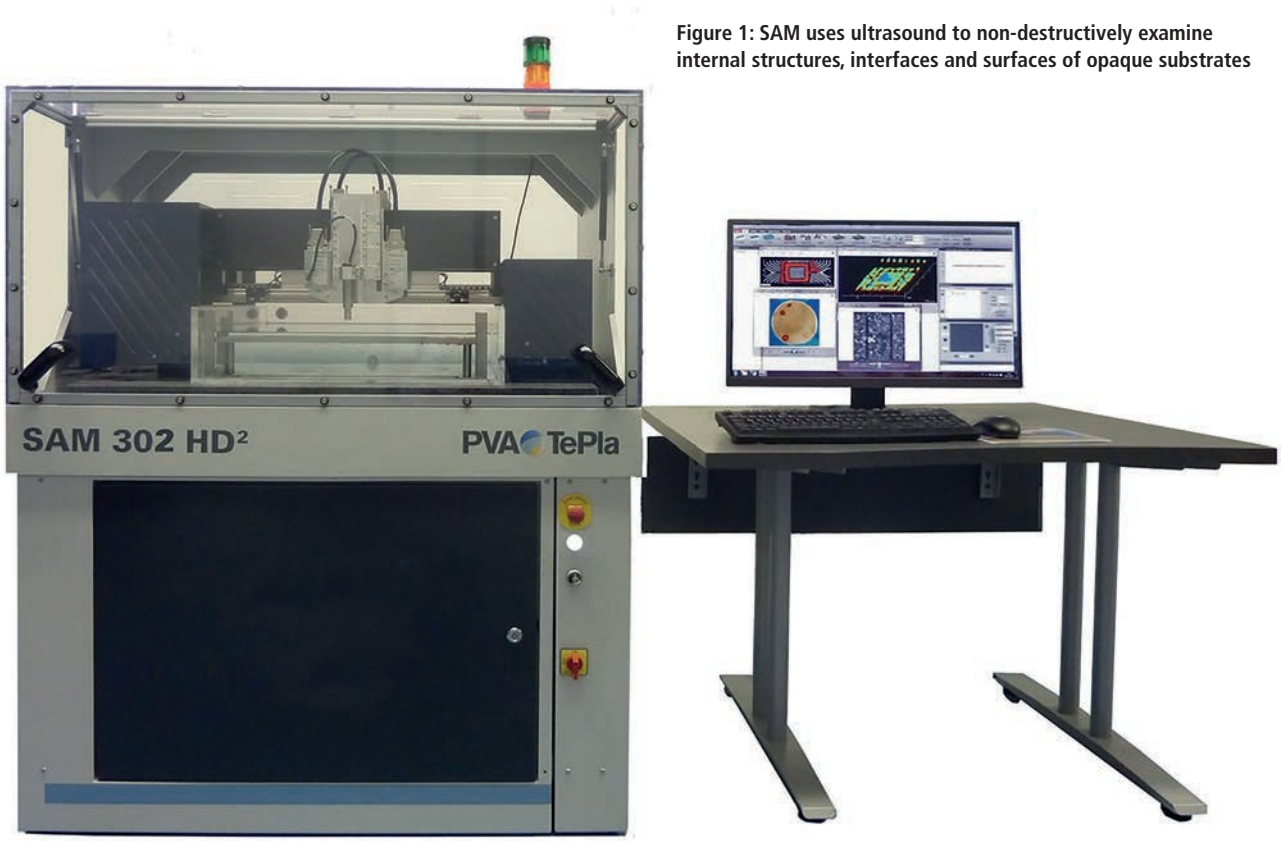

Figure 1: SAM uses ultrasound to non-destructively examine internal structures, interfaces and surfaces of opaque substrates

www.electronicsworld.co.uk

December 2018/January 2019

Electronics WORLD

T&M SUPPLEMENT

THE ESSENTIAL ELECTRONICS ENGINEERING MAGAZINE

Next Generation in Precision...

Contents

Real-time vs common spectrum analysers

By Boris Adlung, Rigol Technologies

RF technology is increasingly being harnessed to send data from a device under test (DUT) to a receiver. For Internet of Things (IoT) applications, the most common way is to use standards like Bluetooth, Wi-Fi or Zigbee. Data from a test system is modulated to an RF carrier via complex modulation schemes, a process that results in very fast and dynamic signal transfer.

Analyser Techniques

The complete RF input signal is shifted to an intermediate frequency via a swept local oscillator using a superposition technique. This means that a signal trace from a spectrum analyser (SA) will sweep between start and stop frequencies according to the adjusted centre frequency and span (which determines the frequency range for which an amplitude is plotted).

Spectrum analysers have auto-coupled sweep time that automatically chooses the fastest allowable sweep time based on several parameters, including RBW (resolution bandwidth, which determines the instrument's ability to resolve signals of equal amplitude), VBW (video bandwidth, a factor that affects the displayed trace quality of a spectrum analyser) and span. The technology is used for fast overview of a wide spectrum with good amplitude accuracy, and for insertion loss or loltage standing wave ratio (VSWR) measurements. Additionally, a common SA is a very useful tool to perform RF measurements with a large dynamic range and good performance.

For measurement of low-level signals, it's important to have good dynamic range. Some standards have reference sensitivity below -120dBm, lower than the noise level. Therefore, a test device needs a noise level as low as possible. This is important, because in an SA, blind time occurs when signal information is lost; see Figure 1.

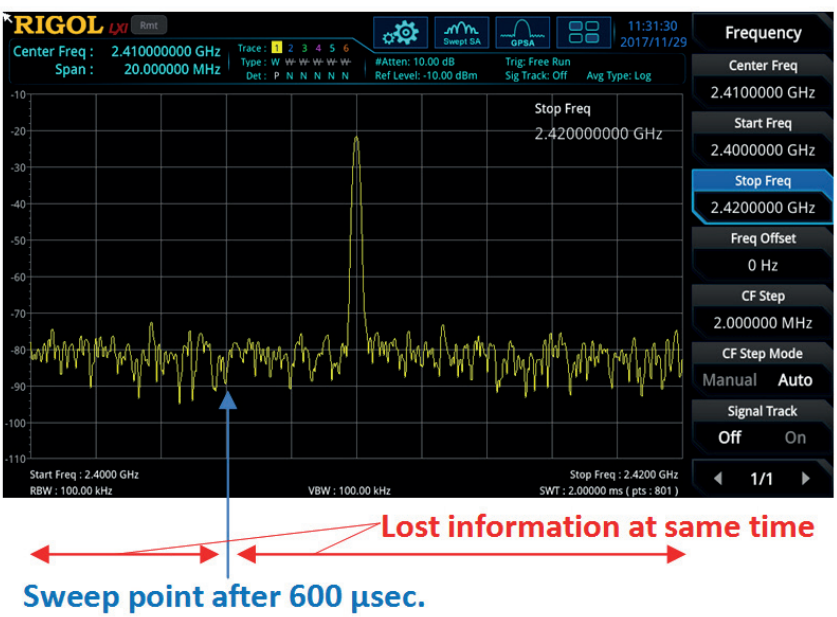

Figure 1: Sweep result of a spectrum analyser with blind time

Bluetooth Example

Random and very fast signals can't be easily detected. However, a fast-changing frequency-hopping signal like Bluetooth can be measured with an SA, with one trace set to maximum hold, and a second to clear write.

It is not possible to capture all signal components with one sweep; several sweeps are necessary, and they are only visible with the maximum hold function; see Figure 2. However, not all frequency components are visible, there's no time information available, and it's not possible to determine if it is a frequency-hopping spread-spectrum signal.

Frequency, span and RBW have a direct influence on the sweep time in common spectrum analysers. If a better frequency resolution is required, then RBW needs to decrease, which results in slower sweep time and more difficult and time-consuming capture of fast signals.

Real-time spectrum analysis uses Fast Fourier Transform (FFT) technology and works without a sweep and with a different calculation format. In a normal FFT form, the calculation time is longer than the FFT process, which results in loss of information because of the gap between FFT acquisitions; see Figure 3. This type FFT analysis can't be used for measuring pulsed signals, because parts of the pulse may fall into the gap between FFT acquisitions, resulting in a different frequency for each pass.

In real-time acquisition, the calculation

Figure 2: Bluetooth signals are only visible via the SA's maximum hold function

is performed in parallel to the FFT process, and is very fast – faster than the FFT acquisition. Display data changes constantly and fast, resulting in time acquisition of different FFT blocks being gap-free; see Figure 4. Also, the speed won't change with different RBW adjustments.

Gap-Free FFT Example in A Real-Time Operation

A fixed number of samples (1024) is used for one FFT time acquisition. Each FFT calculation uses a window function – windowing is important to define a discrete number of time points for the calculation.

The size of the window can be varied, and is not fixed in the time domain. Varying the window size will affect the real-time resolution bandwidth; or, putting it another way, with changing RBW, the size of the window will also change.

The slew rate and number of window points influence the leakage (operations create new frequency components referred to as spectral leakage), frequency and amplitude accuracy. The downside of using a filter is that some signal information will be lost due to amplitude suppression at the beginning and end of the filter; see Figure 5.

The position of a time signal like a pulse needs to be in the centre of an FFT window to be correctly transformed into a frequency range. If a pulse falls between two FFT events, its amplitude is suppressed by the filter side loops and is no longer correct; see Figure 6.

Some instruments, such as Rigol's RSA5000 series, use overlapping FFT events to avoid losing signal information. This has the effect of covering a greater spectrum over a given period and the time resolution is better. Smaller events can also be measured (Figure 7), and any signal suppression due to windowing is eliminated.

It's obvious that the overlapping process of FFT events directly influences the shortest of pulse widths, which can be measured with a real-time spectrum analyser. The overlapping of FFT frames is not possible during calculation, but the overlap time of FFT frames can be calculated with the following formula:

$$T_{overlap} = T_{acq} - T_{calc}$$

For example, for a sample rate of 51.2MSps, the overlap is 13.18µs, or 65.86%, which results in overlap of 674 sample points.

Probability of Intercept

Probability of intercept (POI) specifies the shortest pulse duration that can be measured with 100% amplitude accuracy. Furthermore, POI defines the minimum pulse-width where each pulse will be captured; see Figure 8. Such short pulse events can't be measured continuously with a common SA, and typically require an RT-SA.

POI depends on the FFT rate, used RBW and adjusted span. The principle

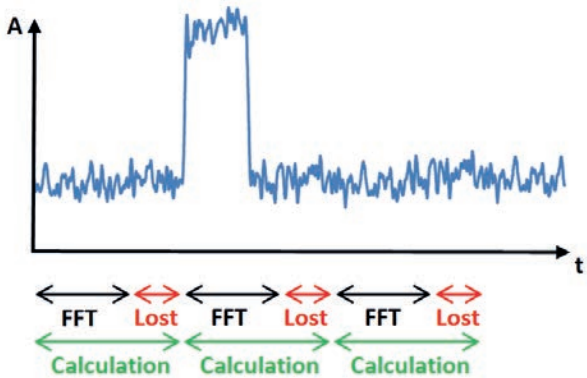

Figure 3: FFT with gaps in between, based on a slow calculation process

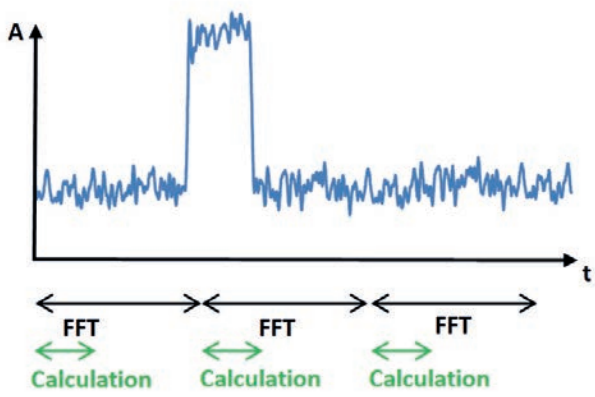

Figure 4: FFT in a real-time spectrum analyser without gaps

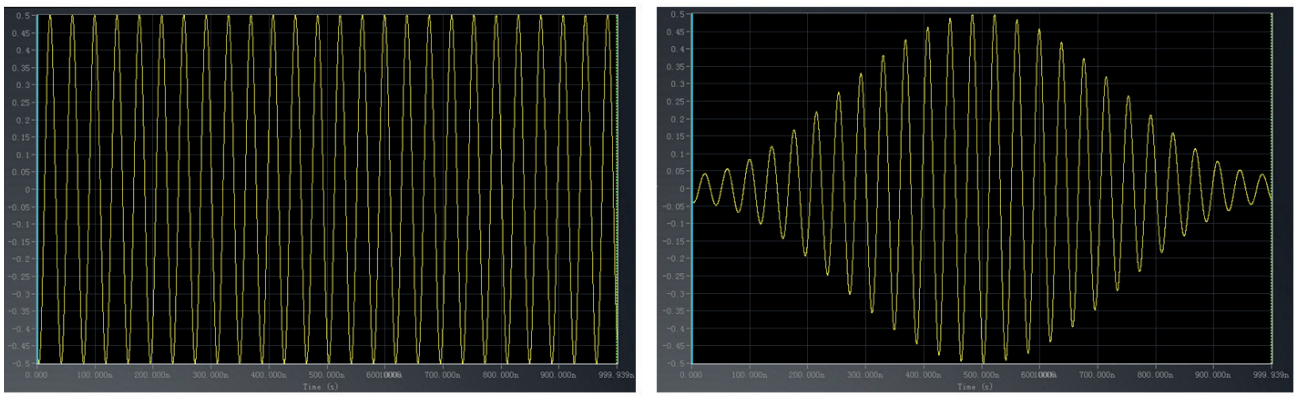

Figure 5: Unfiltered (left) and filtered (right) time signal with lost amplitude information

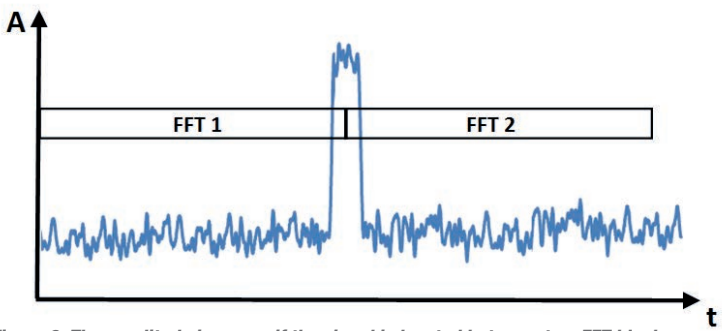

Figure 6: The amplitude is wrong if the signal is located between two FFT blocks

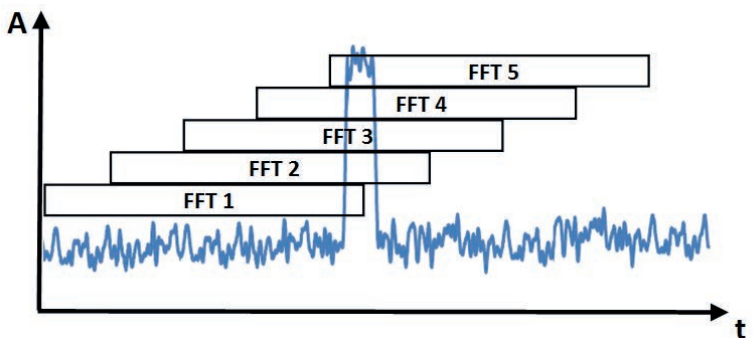

Figure 7: Overlapping process in a real-time spectrum analyser

of POI is described with a span of 40MHz (= 51.2MS/s) and RBW of 3.21MHz (Kaiser window) in Figure 9. Due to the calculation time, a second FFT acquisition starts after 6.82µs. The window size depends on RBW in real-time mode, thus:

$$T_{Window} = \frac{1}{RBW}$$

The start of the first FFT acquisition and the end of the second FFT acquisition define the POI time.

POI can also be calculated with:

$$T_{POI} = \frac{[(N]_{Window} + N_{Fix} - 1) - N_{Overlap}}{Sample\,rate} =$$

$$\frac{(32 + 1024 - 1) - 674}{51{,}2\frac{MSa}{sec.}} = 7{,}45\ \mu sec.$$

Having POI and the speed determined, it is now possible to measure a Bluetooth signal with the RT-SA mode; using maximum hold is no longer necessary.

Density Analysis

Density analysis shows the same results as normal trace analysis, but, with it, a signal's repetition rate can be also analysed.

In normal and density modes it is possible to activate a spectrogram measurement, which is a waterfall measurement frequency over time, measuring the duration of pulses, like Bluetooth signals, for example. With a waterfall spectrogram, signal on/off scenarios can easily be analysed. Density analysis combined with a spectrogram is equivalent to a 4D measurement: power over frequency over repetition rate and power over time; see Figure 10 for a Bluetooth example.

In Power vs time (PvT), it is possible to display a signal's time domain within adjusted real-time bandwidth. The acquisition time can be changed in this measurement. The PvT analysis is displayed for real-time bandwidth used, and not RBW like with an SA with zero-span configuration. Signal bursts of modulated signals and pulses can be displayed to measure their duty cycle and amplitude, or to display pulse trains over a certain period. PvT can be used in combination with normal trace analysis (frequency spectrum) and a spectrogram; see Figure 11.

Comparing the measurement results for a Bluetooth signal in Figures 10 and 11 with that of an SA in Figure 2, a test engineer now has much more information available. Within the adjusted real-time bandwidth,

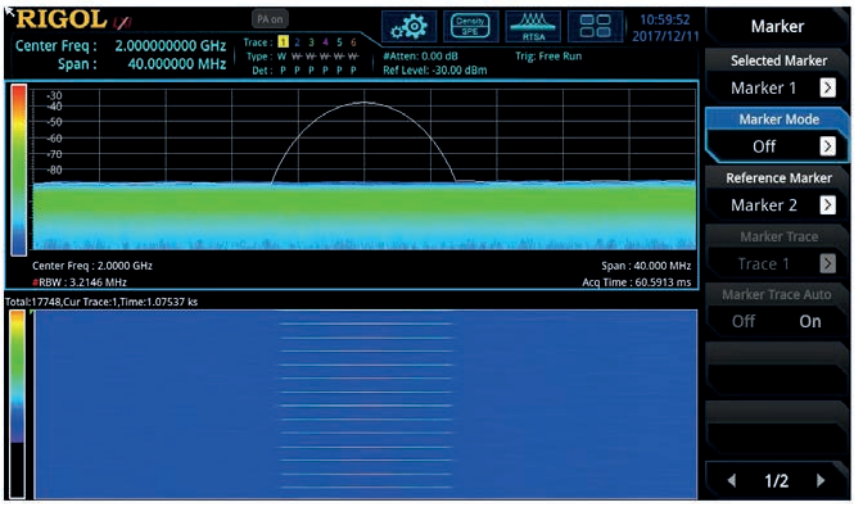

Figure 8: Measurement of a 7.45µ pulse (or period of 1s), with -35dBm amplitude. Each pulse is captured with the correct amplitude

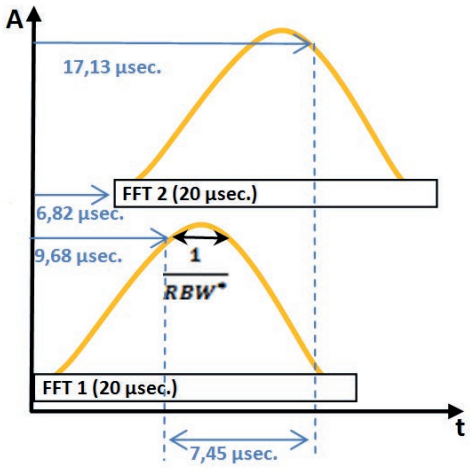

Figure 9: Example with RT-span of 40MHz, sample rate of 51.2MS/s and RBW of 3.21MHz (Kaiser filter)

all frequency components can be measured, and time information can be displayed in parallel with spectrum measurement.

In a spectrogram, it's clearly visible that the signal is a frequency-hopping spread spectrum one, and the length of data blocks can be easily analysed. PvT no longer depends on RBW like with an SA, and the frequency and time domains can be displayed at the same time. ❖

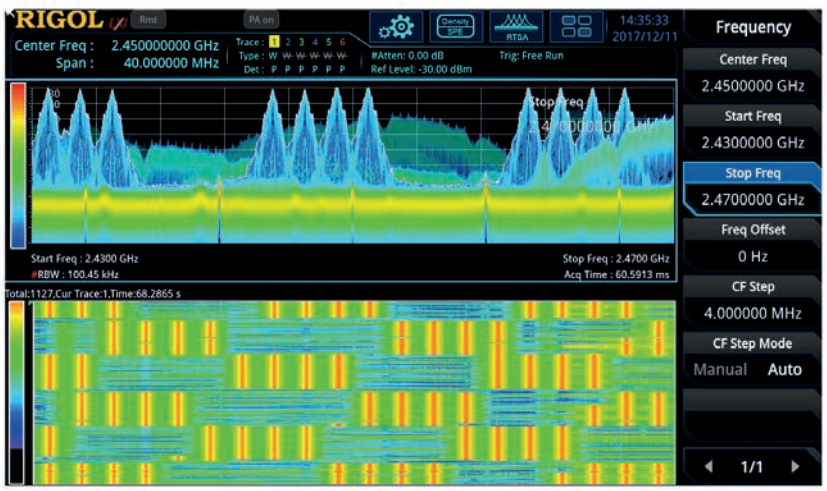

Figure 10: Bluetooth signal measured with density spectrogram

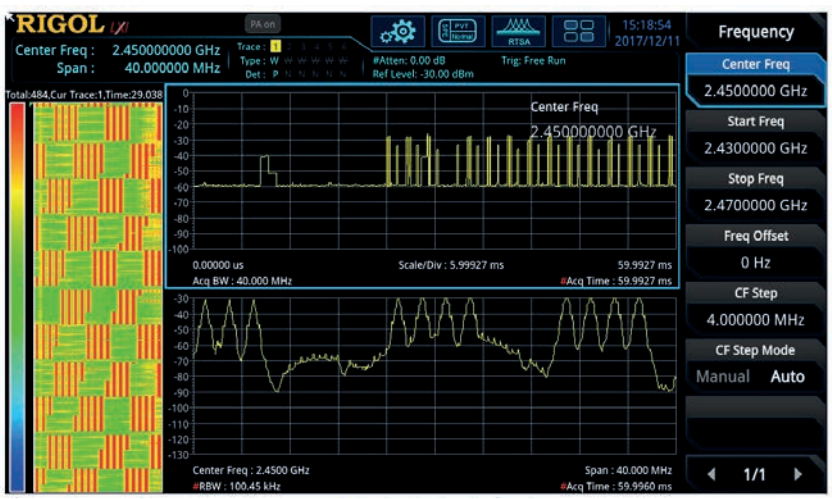

Figure 11: Normal trace vs spectrogram vs PvT of a Bluetooth signal

Real-Time Spectrum Analyser RSA5000 Series

Rigol's new Real-Time Spectrum Analyser RSA5000 series combines an elegant design with full flexibility and speed during test.

The RSA5000 series can be switched between a common s uperposition spectrum analyser (SA) and a real-time spectrum analyser (RT-SA). Its displayed average noise level (DANL), another term for the noise floor of the instrument given a particular bandwidth, is specified as -165dBm/1Hz (typ). Its smallest Probability of Intercept (POI) is 7.45µs.

The RSA5000 can measure an events as short as 25ns.

The instrument provides different measurement modes:

- Normal trace analysis;
- Density analysis;
- Spectrogram;
- Power vs time (PvT).

Top five benefits of 5G New Radio

By Alejandro Buritica, Semiconductor Marketing Specialist, National Instruments

The new air interface, dubbed 5G New Radio (NR), is being developed to support a wide variety of services and devices on 5G; it promises to provide significant benefits for mobile networks, including improved performance, flexibility, scaleability and efficiency.

With the 5G rollout in the UK set for 2020, companies have already started to invest in this technology. Ericsson recently struck a deal with T-Mobile to provide its latest 5G New Radio hardware and 3GPP (3rd Generation Partnership Project) for $3.5bn. However, as companies around the world continue to work on introducing 5G, they are faced with numerous technical design challenges.

Here are the top five technical benefits that 5G NR provides, looking at how this global communication standard will deliver reliable, data-rich and highly-connected applications.

5G NR Waveforms

CP-OFDM: Downlink and Uplink

Recently, researchers have been investigating different multicarrier waveforms, proposing them for 5G radio access. Waveforms that use orthogonal frequency division multiplexing (OFDM) work well for time division duplex operation. They support delay-sensitive applications and have demonstrated successful commercial implementation with efficient processing of ever-larger bandwidth signals. Also, the high spectral efficiency and multiple-input, multiple-output (MIMO) compatibility that OFDM signals can achieve helps meet the extreme data rate and density coverage needs of a new global cellular communications standard.

> *"With the 5G rollout in the UK set for 2020, companies have already started to invest in this technology"*

Furthermore, thanks to channel estimation and equalisation techniques, OFDM waveforms show great resiliency against frequency-selective channels. By attaching a copy of the end of the OFDM symbol to the beginning of the symbol (a cyclic prefix), a receiver can better tolerate synchronisation errors and prevent inter-symbol interference; see Figure 1. The 3GPP settled on using the cyclic prefix OFDM (CP-OFDM) as the waveform of choice for 5G downlink and uplink, with modulation schemes up to 256-QAM.

DFT-S-OFDM: Higher Efficiency Uplink

OFDM waveforms suffer from high peak-to-average power ratio (PAPR). Because the RF power amplifier consumes the most power within a mobile device, system designers needed a type of waveform that could support high-efficiency amplifier operation while meeting the spectral demands of 5G applications. As a result, for uplink, NR offers user equipment (UE) the option of CP-OFDM or a hybrid format waveform called Discrete Fourier Ttransform Spread OFDM (DFT-S-OFDM). Based on this technology, the transmitter modulates all subcarriers with the same data, and it incorporates a lower PAPR with the multipath interference resilience and flexible subcarrier frequency allocation that OFDM provides.

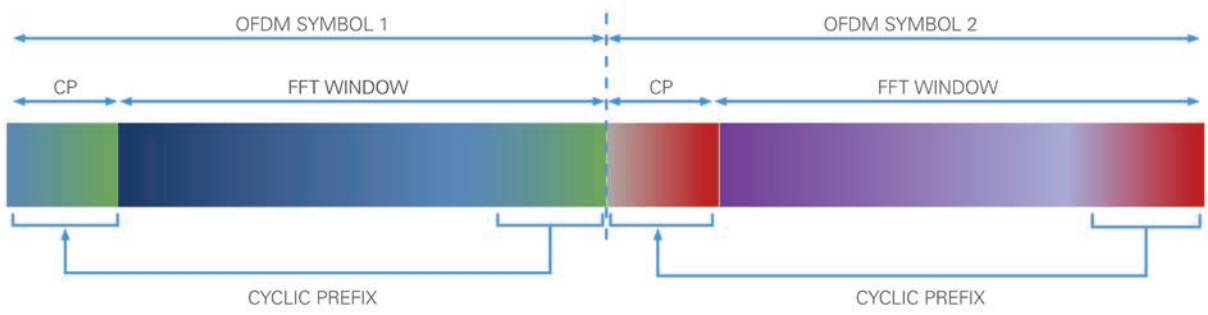

Figure 1: A cyclic prefix separates OFDM symbols – a good example of best-practice development process

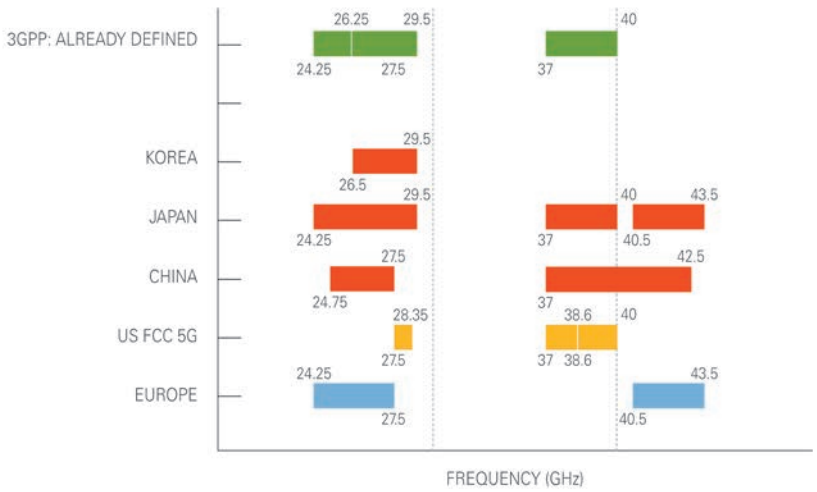

Figure 2: 3GPP-defined and locally adopted bands for NR above 6GHz

Flexible Subcarrier Spacing and Frame Structure

Multiple frequency bands ranging from existing cellular bands (< 3GHz) to wider bands between 3GHz and 5GHz, and up to the millimeter wave (mmWave) region of the spectrum, represent a completely new aspect of 5GNR. Figure 2 shows the current bands defined for NR operation above 6GHz.

As the carrier frequency increases, so does the system phase noise. For example, looking on the carrier phase noise plot of Figure 3, the difference in phase noise between a carrier at 1GHz and 28GHz is about 20dB. This phase noise increase would make it very difficult for a receiver to demodulate OFDM waveforms with the narrow, fixed subcarrier spacing (SCS) and symbol duration of LTE at mmWave frequencies.

Additionally, in mobility scenarios, the channel coherence time decreases as the carrier frequency increases, due to Doppler shift effects. Therefore, at higher carrier frequencies the system has less time to measure the channel and finish a single slot transmission. Using a narrow subcarrier spacing at mmWave frequencies would result in very high error vector magnitude (EVM) and considerable performance degradation.

The 3GPP standardised on a flexible subcarrier spacing approach that scales the space between orthogonal subcarriers, starting with the 15kHz subcarrier spacing of LTE; see Figure 4. One of the fundamental reasons for leveraging the LTE numerology has to do with the ability of NR deployments to coexist and be time-aligned with LTE networks during the first deployments.

The NR subcarrier spacing scales according to the following formula:

$$SCS = 15 \cdot 2^{\mu} KHz, \ \mu \in \{0,1,2,3\}$$

The smallest physical resource block (PRB) consists of 12 subcarriers. Figure 5 illustrates the NR channel PRBs and guard bands.

More Scaleable and Flexible Frame Structure

5G NR has a flexible frame structure. NR slots have 14 OFDM symbols (although there is a special case for 60kHz SCS with an extended CP and twelve OFDM symbols). Since OFDM symbol duration has an inversely-proportional relationship with SCSs, the duration of the slots scales down as SCS increases. The frame structure numbers the slots and groups them into subframes of 1ms duration. Figure 6 shows the standard NR slot and frame structure.

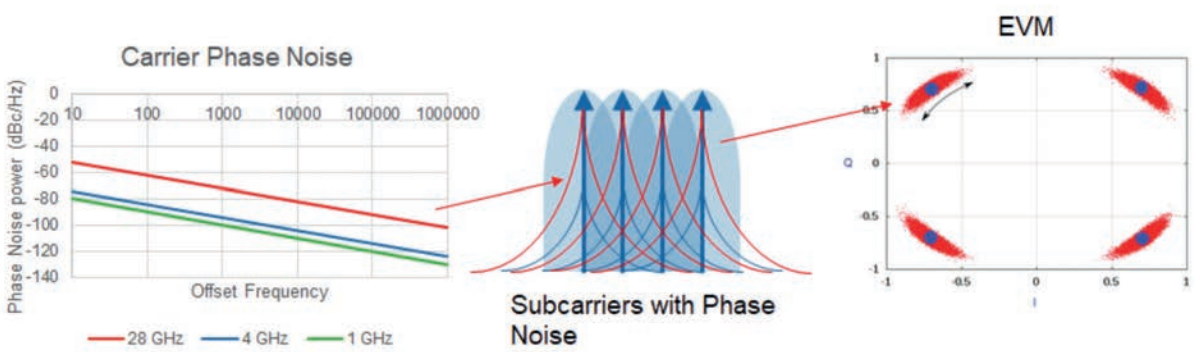

Figure 3: Effect of phase noise on error vector magnitude

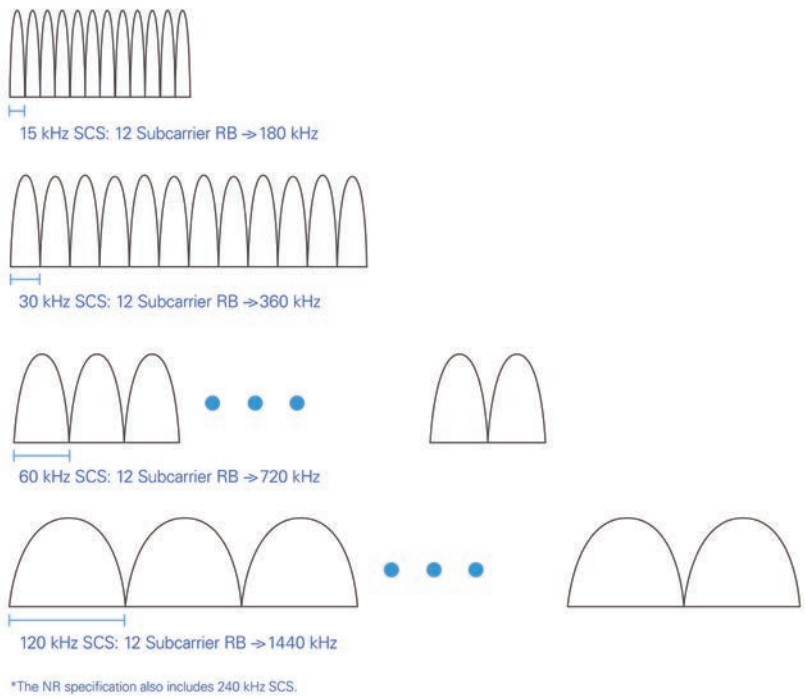

Figure 4: Flexible subcarrier spacing

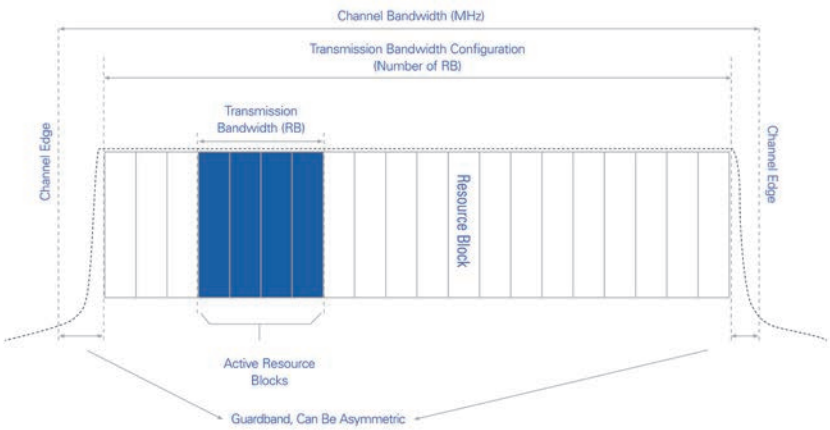

Figure 5: NR channel divided into resource blocks

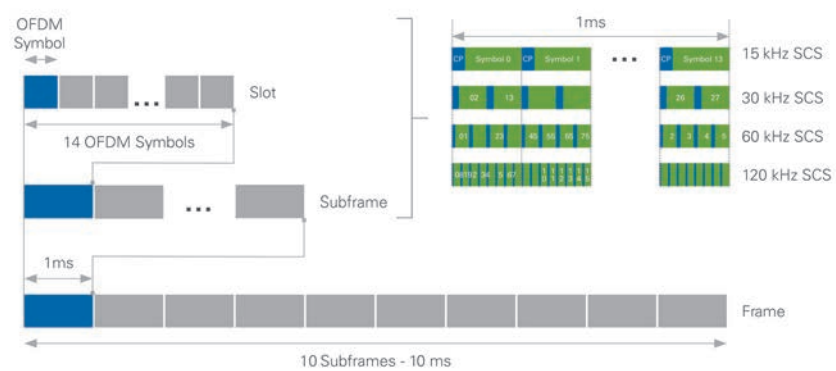

Figure 6: NR frame structure

MIMO

5G NR plans to take full advantage of the distributed and uncorrelated spatial location of multiple users to multiplex users in space and increase the spectrum efficiency. Thanks to multi-user MIMO (MU-MIMO) technology, the gNB (base station) sends simultaneous data streams to different users, maximising the signal strength at each user's location, while presenting minimum signal strength (a null) in the directions of the other receivers. Consequently, the gNB talks to multiple UEs independently and simultaneously, as Figure 7 shows.

Massive MIMO for 5G

A Massive MIMO configuration takes place when a system has many times more gNB antennas than the number of UE per signalling resource. The large number of gNB antennas relative to the number of UE can create huge gains in spectral efficiency, and enable the system to serve many more devices simultaneously within the same frequency band, compared to today's 4G systems. National Instruments (NI), along with industry leaders such as Samsung, continues to demonstrate the viability of Massive MIMO systems with its platform of software-defined radio and flexible software for rapid wireless prototyping.

MmWave for 5G

5G systems operating at 28GHz or above have the benefit of having more available spectrum for larger channels. Although there is less spectral crowding at these frequencies than below 6GHz, there are very different propagation effects, such as higher free-space path loss and atmospheric attenuation, weak indoor penetration and poor diffraction around objects.

To overcome these undesirable effects, mmWave antenna arrays can focus their beams and take advantage of the antenna array gain. Fortunately, the size of these antenna arrays decreases as the frequency of operation increases, allowing for a mmWave antenna array with many elements taking up the same area space as single sub-6 GHz element, as shown in Figure 8.

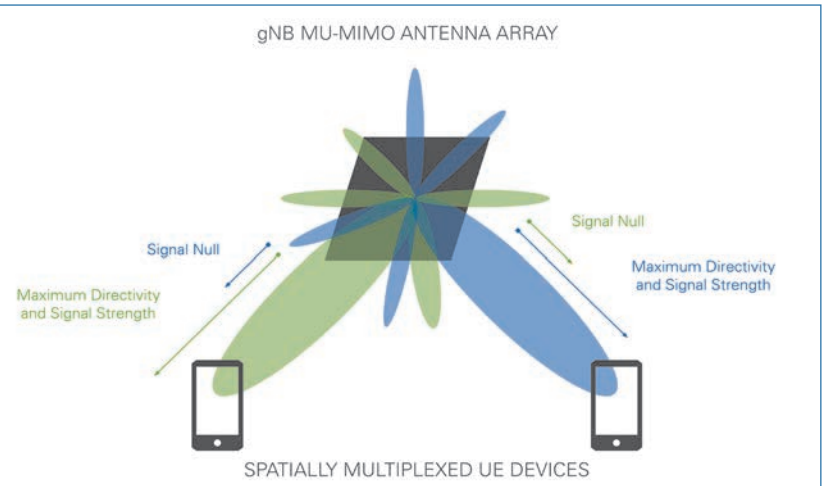

Figure 7: MIMO beamforming for spatial multiplexing

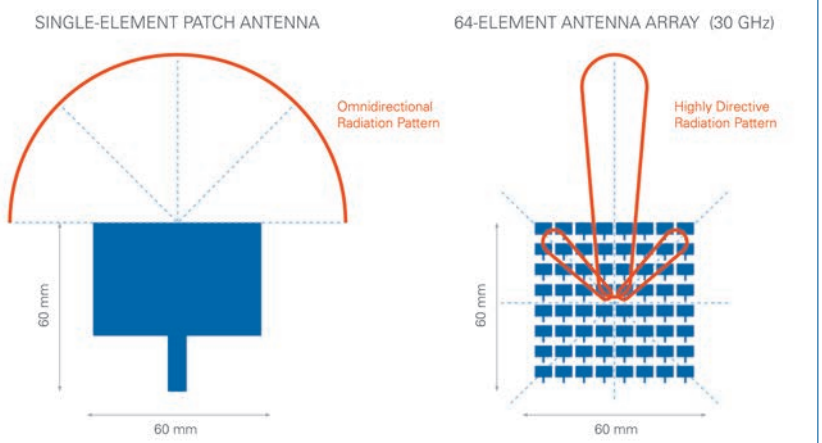

Figure 8: Comparison of mmWave and sub-6GHz antenna arrays

The channel coherence-time decreases significantly at mmWave frequencies, placing tough restrictions on mobility applications. Researchers continue to investigate new ways to improve UE mobility at mmWave frequencies, but most likely the first 5G mmWave systems will serve fixed wireless access applications, such as backhaul, sidelink and static home connections.

Bandwidth Parts

In the future, a wide range of 5G applications will need to operate successfully across many different bands with varied spectrum availability.

An example is a situation in which a UE with limited RF bandwidth operates alongside a more powerful device that can fill a whole channel using carrier aggregation, as well as a third device that can cover the whole channel with a single RF chain.

Wide bandwidth operation has a direct effect on the data rates that users can experience, but it comes at a cost. When UEs don't need high data rates, using wide bandwidth leads to inefficient use of RF and baseband processing resources. However, 5G NR introduces the new concept of bandwidth parts (BWPs) where the network can negotiate for certain UE to occupy one wideband carrier, and, separately, it can configure another UE with a subset of contiguous resource blocks. This creates a greater diversity of devices with varying capabilities sharing the same wideband carrier. This kind of flexible network operation that adjusts to a UE's differing RF capability does not exist in LTE.

Figure 9 shows the allocation of two BWPs (BWP 1 and BWP 2) to one UE, while reserving a third, full-channel, overlapping BWP (BWP 3) for potential use by another higher-bandwidth UE or application.

For example, using BWPs, NR can support UEs with narrow RF capabilities and reduce energy consumption when a device doesn't require full bandwidth operation.

Into the Future

Thanks to higher bandwidth channels and multiple numerology options, NR systems will operate in both sub-6GHz and mmWave bands with appropriate handling of multi-path delay spread, channel coherence time and phase noise.

Latest developments in massive MIMO and beamforming technology will enable NR to maximise spectral efficiency and guarantee better quality of service for more users. Additionally, considering the commercial practicalities of deploying different UEs with different RF capabilities, the new concept of BWP in NR will lead to more energy-efficient UE operation and superior spectrum management. And with less than two years until the UK rollout of 5G, creating the next generation of 5G devices presents a significant design and test challenge. However, one thing we do know is that employing a platform-based approach to design, prototype and test wireless technologies will be a key factor in turning 5G into reality within the next decade. ❖

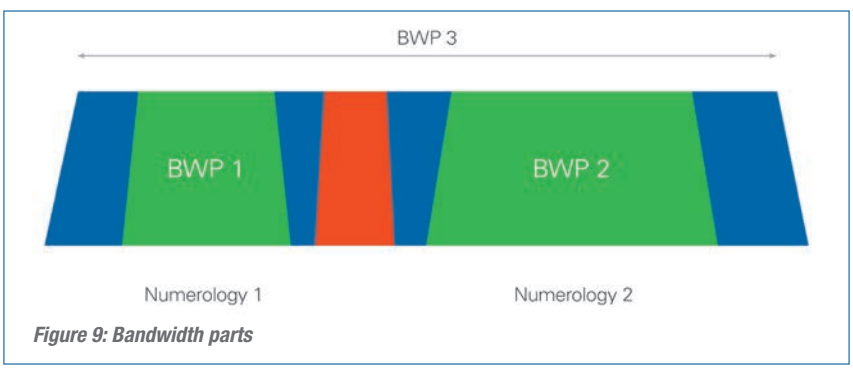

Figure 9: Bandwidth parts

New applications drive increased accuracy in power measurement

By Anoop Gangadharan, Product Marketing Manager, Yokogawa Europe

As markets for power electronics expand and grow, so does the need for their reliable testing, enhanced safety, efficiency and performance. In sectors as diverse as renewable energy and electric vehicles, there's growing need for custom measurements and consistent accuracy, buoyed by application diversity and standards. Engineers need test and analysis platforms that deliver reliable measurements today but are also prepared for the challenges of tomorrow.

For example, in the automotive sector, electric vehicles require greater charging capacity, shorter charging times and extended travelling range, which requires positive and negative cycle evaluations of these vehicles' battery charge-and-discharge characteristics. Similarly, the evaluation of inverter signals needs to account for the harmonic superimpositions from switching circuits. Minimising interference from switching noise requires isolated inputs, high-speed sample rates and long-term observations; see Figure 1.

Nowadays there are also moves toward contactless charging, meaning such evaluations will need to be done at lower power factors (the ratio of actual electrical power dissipated by an AC circuit to the product of the r.m.s. values of current and voltage) and frequencies of hundreds of kilohertz – parameters presently outside the scope of traditional test instruments.

Equally, there are very high speed power devices made of semiconductor materials such as silicon carbide and gallium nitride that are increasingly found in power-conversion products (inverters, drives, etc). This results in common-mode voltage effects that can create noise problems that affect the performance of the measurement systems.

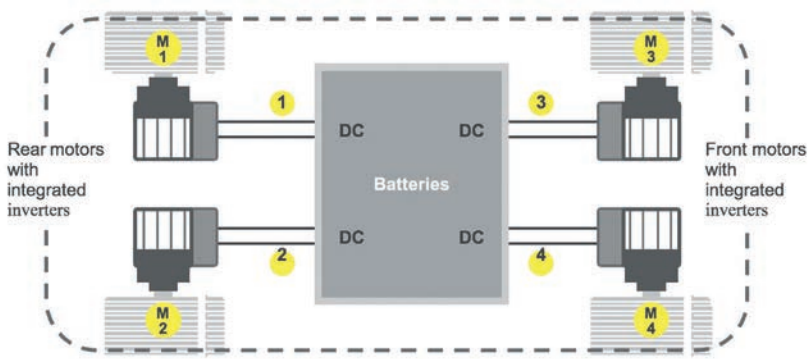

Figure 1: Measuring powertrain efficiency in an electric vehicle, showing four DC measurements (1-4) with the corresponding mechanical power measurements (M1-M4)

Power Distribution

In power transmission and distribution too there are new developments, including renewable energy stations and energy-positive buildings and infrastructure, where

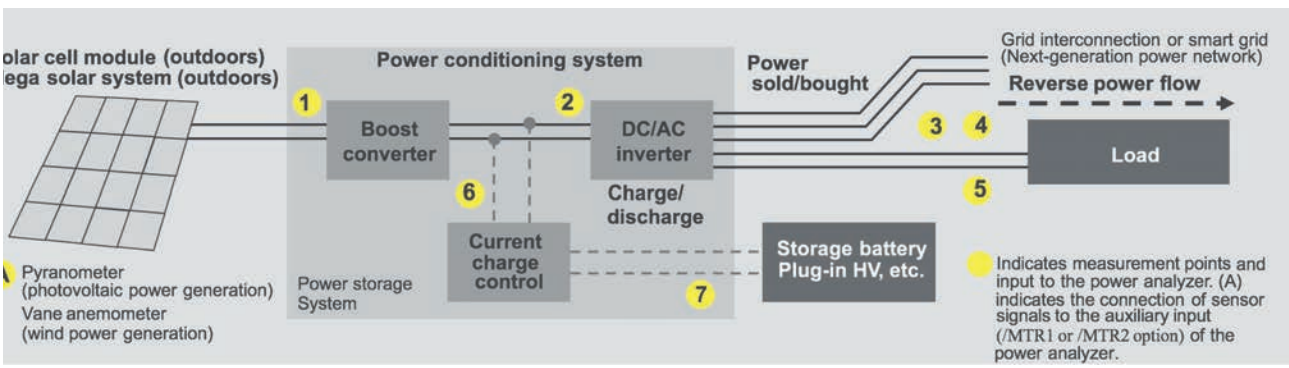

Figure 2: A precision power analyser helps engineers of renewable energy grids to improve conversion efficiency by gaining precision insights into charging, discharging, storage and overall system efficiency

Figure 3: A Yokogawa WT5000 is configured for simultaneous synchronised measurements from four torque and rotation sensors to determine the overall efficiency of four motors

there's no longer unidirectional electricity flow from power station to consumer; see Figure 2. With a multitude of renewable and non-renewable power stations feeding the power network, a balanced grid needs robust testing and accurate measurements, to reduce the impact of noise, distortion and harmonics from multiple sources.

Power stations and large consumers also need to evaluate the effects of their power outputs and usage levels on the grid and on other users. Highly accurate instruments will also be needed for high-frequency measurements. With mean voltages differing greatly from the fundamental voltage waveform, harmonic measurements are needed to establish the values of derived measurements, such as active power.

Similarly, addressing the challenges of measuring parameters such as energy efficiency, harmonic content and power factor will require both progressively greater accuracy and consistency in measurement over the specified ranges and conditions.

Addressing the Challenges

These challenges are now being addressed by a power analyser, the Yokogawa WT5000 (Figure 3), which sets new standards in terms of precision and accuracy. Its flexible modular architecture allows customisation, which can meet the needs of different applications.

This instrument offers a high degree of isolation, noise immunity, current sensing and filtering in a modular architecture that provides an extensible measurement platform. Its ±0.03% power accuracy is combined with a frequency range of 5MHz and 10MS/s (18-bit) sampling rate. Current measurements are available via 5mA to 5A or 0.5A to 30A modules.

> *"Specialised measurement solutions are required to prove adherence to the stringent criteria set by manufacturers' internal standards and by external standards"*

Seven built-in slots for user-swappable power input modules and diverse mainframe options enable users to expand or reconfigure the instrument as their applications and requirements change. In addition to on-power parameters, torque and frequency from four separate motors can also be measured.

Automotive Applications

Between 16% and 18% of the total charge of an electric car is consumed by losses in the electric drive system. Electric and hybrid car manufacturers therefore need to accurately evaluate motor and inverter control to achieve higher precision and greater efficiency. In addition, the accurate analysis of inverter waveforms without interference from switching noise is a key part of evaluating the motor's drive circuit.

The most important test requirements here are multi-phase measurements from battery, inverter and motor; evaluation of motor characteristics such as torque, rotation speed and direction, slip and electrical angle; battery charge-and-discharge characteristics; and harmonic analysis of inverter signals at various rotation speeds.

With high accuracy, multi-channel power measurements, evaluation of up to four motors and harmonic comparison capabilities, the WT5000 precision power analyser helps automotive engineers improve conversion efficiency, shorten charging times and improve driving range. Its guaranteed accuracy in multichannel measurements enables simultaneous measurements of voltage, current, power, torque, rotation speed, electrical angle and mechanical power, allowing complete evaluation of motor performance and mechatronic efficiency.

With the ability to measure harmonics up to the 500th order, even at low rotation speeds, the instrument also supports harmonic analysis without an external sampling clock.

Figure 4: The WT5000 has seven built-in slots for user-swappable power input modules

Automotive Case Study 1

One major automotive manufacturer is carrying out extensive simulations on test rigs to analyse these key parameters. To ensure higher performance and efficiency of the vehicle powertrain, these tests are carried out under rigorous conditions, including industrial inverters and heavy motor loads in simulated extreme conditions (700VDC), far greater than in the real world (< 500V). During these stress tests, analysis is carried out on multiphase voltages, currents and mechatronics parameters with the engine connected to a test rig consisting of an industrial inverter and rotating loads to simulate the car's inverter and wheels, respectively.

Since the engine powers two electric motors that rotate the front and rear axles, multichannel electromechanical measurements were needed of the inverter and two three-phase motors under extreme voltage, power and torque. As the test rig generates the relevant torques and speeds to simulate the electric drive train, some of the parameters measured include:

- Line and phase voltages across the 3-phase power system;
- Rotational speed, torque and slip;
- Harmonic evaluation of inverters at high switching speeds;
- Engine efficiency.

To achieve the best efficiencies, parameters such as battery voltage, cooling fluid temperature, influence of torque and others are modified and tweaked.

With current varying from a few to several hundred amperes, it is important to have not only a wide dynamic range for measurements, but also high crest factors for capturing any unexpected peaks or distortions.

With such a wide variety of DC and AC signal analyses and electromechanical measurements across various test conditions, specialised measurement solutions are required that can reliably prove adherence to both the manufacturer's internal standards and external ones, such as WLTP, NEDC and NEFZ.

The multiphase voltages, currents and mechatronics parameters through the battery, inverter and motor systems are analysed at different stages of the development cycle using different measurement solutions including Yokogawa precision power analysers for guaranteed accuracy in motor evaluation, plus the company's DL850E vehicle edition Scopecorder to provide thorough analyses of mechatronics and CAN, DC bus and ECU communications signals.

Automotive Case Study 2

To ensure the safety, performance and efficiency of new electric vehicles, another manufacturer needed to extract maximum efficiency from the charging system, power train and components of their vehicle system.

Noise, harmonics, resonance and other parameters were also evaluated within inverters and motors while pushing the vehicles to the limits of their performance to assess the effects of excessive temperatures, voltages or loads.

In addition to tests in actual prototype vehicles, this manufacturer is performing extensive simulations on test rigs to analyse key parameters and to assess their effects under laboratory conditions.

Hence engineers have developed a "hazardous voltage" rig, capable of tests over the ranges 60-1500VDC and 30-1000VAC, although in practice test voltages in this application are normally limited to 200-500V.

The test rig is used to analyse multiphase voltages, currents and mechatronics parameters in the battery, inverter and motor system. Testing the powertrain requires multichannel electromechanical measurements from inputs such as the battery, booster converter and the three-phase motor, along with mechanical measurements from torque and speed sensors. This allows the simultaneous measurement of torque, rotation speed and direction, along with electrical parameters like voltage, current and power, for entire evaluation of charging, discharging and powertrain efficiency.

In this case, the powertrain includes two synchronous permanent magnet electric motors powering the front and rear axles. In the test rig, AC dynamometers, or "dynos", are used to absorb and generate the relevant torques and speeds, thereby simulating the entire electric drive train of the vehicle. Tests are conducted to provide reliable measurements of:

- Line and phase voltages across the 3-phase power system;
- CAN, DC bus and ECU automotive Ethernet communications;
- Trigger and excitation voltages;
- Rotational speed, torque and slip;
- Harmonic evaluation of inverters at high switching speeds.

Again, by analysing individual components, systems and subsystems individually and combined, engineers can achieve significant improvements in the powertrain and charging systems for greater performance, torque, charging time and driving range. ❖

SOUTHERN 19 Manufacturing & Electronics

FARNBOROUGH | Hants | GU14 6XL

Southern Manufacturing & Electronics poised to be a successful 2019 event

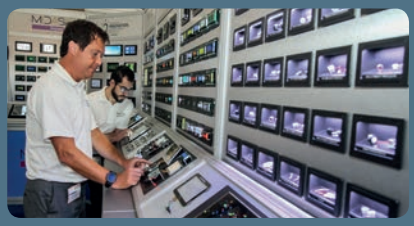

Southern Manufacturing & Electronics, the UK's top annual electronics and industrial technology show, returns to Farnborough on February 5-7th, 2019.

The move to a new permanent venue in 2018 was a milestone in this event's two-decade track record and the main drive behind its additional growth in 2019.

Exhibitor bookings for February are already up by 20% compared to a year ago, with a 26% increase in bookings from overseas vendors, confirming the exhibition's wide international appeal and the variety of products and solutions it'll offer.

With around 22% of the UK's 3,400 aerospace enterprises and a significant number of automotive, medical technology, marine and high-tech manufacturing companies, Southern Manufacturing & Electronics is a comprehensive and popular marketplace for components and services. The show is also an extremely important platform for subcontract services such as PCB and contract electronics manufacture. In this sector too, the show offers an impressively wide attendance, from UK firms to partners from Eastern Europe and Asia.

Wider-Spanning Exhibition

Electronics is only one element of a much wider exhibition that shows an array of manufacturing-related content. Technology trails help delegates around the exhibition, enabling them to make the most efficient use of their time at the show. Dedicated areas like the Machinery Zone, for example, enable visitors to quickly pinpoint their areas of interest. A snapshot of offerings on display in 2019 includes automation, CNC machine tools and machining centres, CAD/CAM tools, advanced adhesives, fasteners and joining technology, laser cutting, packaging solutions, labelling and marking, pressings, fabrications and enclosures, metrology and test equipment, coating and finishing, motors, drives and controls and handling and storage solutions.

Away from the exhibition and demonstration areas, the free technical seminar programme is always an extremely popular feature, running throughout the three-day show in two theatres. The programme for 2019 provides an extensive lineup of professionals from industry, academia and commerce, bolstered this year by the show's much closer involvement with several key industry organisations such as Composites UK and the Farnborough Aerospace Consortium. The partnerships have given access to authoritative technical knowledge, free to visitors and exhibitors alike via the show's technical seminar programme. Some of the new topics at the 2019 event's programme include a review of incremental sheet forming processes, automated mould design and large-scale 3D printing.

Easy Access

Farnborough International Conference and Exhibition Centre offers free car parking and is well-served by road and public transport links. A regular free shuttle bus service operates directly to the show from both Farnborough mainline railway stations. The venue has high-standard facilities, including free Wi-Fi service and high-quality catering.

Admission to the show is free. More information and tickets are available from www.industrysouth.co.uk, or call Phil Valentine, Managing Director, European Trade & Exhibition Services on +44 (0)1784 880890.

NEW AND OLD NAMES JOIN THE SHOW

- CamdenBoss returns to Southern in 2019, boosted by its recent merger with Smartboxx. The firm will show its greatly enhanced range of enclosures and a UL listed terminal blocks, IP-rated circular connectors and switches.
- New exhibitor Canvys is a specialist in OEM and custom display engineering, designing and manufacturing display products through their entire product lifecycle.
- New for 2019 on the Craft Data stand will be a TFT LCD incorporating the popular HDMI (high definition multimedia interface), and "stretched" or "bar-type" TFT LCDs.
- Components distributor Easby Electronics returns in 2019 with an impressive catalogue of electrical and electronic components from leading brands such as TE Connectivity, Samsung, Faratronic, Ducati, Samwha, Nippon Chemi-Con, Samyoung, Duracell, Vogt, Taiwan Semiconductor, Fagor, Degson, Sunled, ITW Switches, Myrra, Mornsun and JST.
- On stand A125, Luso Electronics will exhibit a wide range of power supply solutions and latest modular configurable units from Excelsys including the fanless-design CoolX range.
- Returning in 2019, the £43m turnover JJS Manufacturing is a substantial UK electronics manufacturing services (EMS) company, specialising in end-to-end procurement, manufacture and supply chain solutions.
- European partners exhibiting in 2019 include Cicor Romania, with a broad range of production capabilities in PCB assembly, system assembly and box building, among others; and Volburg SIA from Latvia, an EMS company.
- Eurocircuits will present a five-day prototype and small series electronics assembly service.

SIGLENT TECHNOLOGIES RELEASES ITS FIRST RF SIGNAL GENERATOR

Siglent Technologies has launched a two-model RF signal generator series, with two operating frequency ranges: the SSG3021X with a maximum output frequency of 2.1GHz and the SSG3032X to 3.2GHz. A bandwidth upgrade can extend the 2.1GHz model to 3.2GHz.

There is a 5-inch capacitive touch display, and support for USB mouse and external keyboard control. Users can easily connect tablets, computers and phones to the SSG using a LAN interface and the built-in web interface.

All analogue modulation types (AM, FM and PM) are included as standard. A pulse train generator is an option. The instrument supports several popular USB power meters for real-time regulation of output power. The SSG3000X-IQE includes all base functions of the SSG3000X, with additional digital IQ-modulation capabilities.

www.siglenteu.com

POWERSOLVE SERIES OF COMPACT, SINGLE-OUTPUT AC-DC POWER SUPPLIES

Powersolve's new PSY280 series of compact, single-output AC-DC power supplies are designed to provide up to 300W across a wide operating temperature range, from -30° to +85°C. The six-model series consists of open chassis units with a tiny 50.8 x 101.6mm footprint and a height of 33.5mm.

Operating from a wide 90-264VAC input range with active PFC, the models provide output voltages from 12VDC to 55VDC, giving 150W convection-cooled, 180W conduction-cooled with baseplate and 250W with fan cooling. With both conduction and forced air cooling, a PSY280 unit will give 300W.

Efficiency is up to 92% and no load power consumption is 0.15W without a fan. The power supplies are protected against short circuit, over current, over voltage and over temperature.

The PSY280 series meet all relevant EMI/EMC standards and full safety approvals are pending.

www.powersolve.co.uk

ALLEGRO AUTOMOTIVE AND HIGH-EFFICIENCY SENSING TECHNOLOGIES

Allegro MicroSystems showed a variety of intelligent solutions at Electronica in Munich last month, giving automotive and industrial manufacturers a competitive edge – including a new coreless current sensor IC.

The ACS37650 IC offers substantial space savings by eliminating the need for a concentrator core in high-current sensing applications, such as electric vehicle traction inverters. The programmable device provides closed-loop sensing, with extremely low noise and high resolution, and operates over an extended automotive temperature range.

Also displayed were Allegro's newest fan and pump motor driver ICs, which feature an embedded FOC algorithm that provides ultra-quiet operation with zero reverse angle start-up.

Allegro's solar offering includes galvanically-isolated surface-mount current sensor ICs.

www.allegromicro.com

MOUSER AND SAMACSYS NOW OFFER FREE PCB FOOTPRINTS, SCHEMATIC SYMBOLS AND 3D MODELS

Mouser Electronics has joined forces with SamacSys, an electronic component library solutions supplier, to provide customers with a range of free design resources, including PCB footprints, schematic symbols and 3D models for over 1.1 million components.

These design resources work seamlessly with top engineering CAD systems, including Cadence, Altium and other programs. The new service will be available free to Mouser customers around the world. More importantly, SamacSys will fully support all Mouser's new product introductions, giving engineers access to a current, high-quality library of PCB footprints, schematic symbols and 3D models for the newest available components.

Mouser's partnership with SamacSys will further complement the technical support, service, tools and resources that Mouser already provides for more than 600,000 customers worldwide.

www.mouser.com/electronic-cad-symbols-models

FINDING THE RIGHT SENSOR FOR THE DESIGN WITH TTI'S NEW GUIDE

TTI, a specialist distributor of electronic components, has published a Sensors Application Guide which, for the first time, is split by market sectors rather than franchise or device type. Sections include smart building and appliances, HVAC, renewable energy, robotics and factory automation, materials handling, EV and automotive, medical, wearables and more.

Here, Honeywell offers a range of gas, air quality, dust and CO_2 sensors through its City Technologies acquisition that solve modern urban challenges. Another franchise, Amphenol Advanced Sensors, offers the Telaire and SGX Sensortech product ranges, which similarly address urban air-quality issues. TDK and TE Connectivity add a portfolio of leaded thermistor and custom temperature probes that work hand-in-hand with air quality monitoring to deliver the correct environment. Signed last year, Sensata, offers ruggedised optical encoders for materials-handling vehicles.

www.ttieurope.com

WORLD'S FIRST-EVER DRONE STANDARDS ARE OUT NOW

The first-ever worldwide standards for the drone industry were released by the International Standards Organisation (ISO) last month.

The long-awaited standards have been developed after several years of collaboration between standards institutions worldwide, and are expected to trigger rapid acceleration of growth within the drone industry. The new standards will play an essential role in guiding how drones are used safely and effectively in a framework of regulatory compliance.

The ISO Draft International Standards for Drone Operations were formally released last month for public consultation, with drone professionals, academics, businesses and the general public being invited to submit comments by 21 January 2019 with final adoption of these standards expected in the US, UK and worldwide in 2019.

Bi-directional 15kW 500V DC programmable power supply

Delta Elektronika has introduced its first 15kW standard power supply offering a bi-directional output and advanced new features at the price of a standard version. Operation is as easy as ever with no need to study bulky manuals.

The SM500-CP-90 features a flexible constant power output characteristic: the lower the voltage, the higher the current: 500V, -30 to +30A, 250V, -60 to +60A and 166V, -90 to +90A. Voltage, positive current and negative current can all be adjusted from zero to maximum. In sink mode Delta's Power Regeneration Technology h an efficiency of 95%. Because of this high efficiency, cabinet height is restricted to just 3U without any compromise on product lifespan. Dynamic response to load changes is excellent allowing very fast load variations between -90 and +90A while all-digital control makes it possible to adapt regulation to match load type. The input range of a standard unit encompasses 380 up to 480V AC rated voltages, covering 86% of the world's electricity grids.The new SM500-CP-90 is protected against all overload conditions while temperature controlled fans guarantee silent operation.

EMC conducted and radiated emissions are according to EN55022 Class B. On paper, the specifications of this power supply may seem beyond what is possible but the SM500-CP-90 exceeds expectations in any application!

Available in the UK exclusively through:-

POWER SOLVE

www.powersolve.co.uk

Tel: 44-1635-521858 Email: sales@powersolve.co.uk

SOUTHERN 19 Manufacturing & Electronics

Incorporating The Subcontract Engineering Exhibition
AUTOAERO
FARNBOROUGH • 5-7 FEBRUARY 2019

FARNBOROUGH | Hants | GU14 6XL

5th – 7th February 2019
9.30am – 4.30pm
(3.30pm close Thurs)

FREE SEMINARS & PARKING

The UK's must-attend event for every industrial engineering and manufacturing professional

Meet over 800 national and international suppliers under one roof in the brand new Farnborough venue next February at Southern Manufacturing & Electronics (inc AutoAero) 2019.

See live demonstrations and new product launches of machine tools & tooling, electronics, factory & process automation, packaging & handling, labeling & marking, test & measurement, materials & adhesives, rapid prototyping, ICT, drives & controls and laboratory equipment.

Free industry seminar programme online @ **www.industrysouth.co.uk**

The exhibition is **free** to attend, **free** to park and easy to get to. Doors open at 9.30am on Tuesday 5th February.

OIL & GAS
DEFENCE
FOOD & DRINK
AUTOSPORT
MARINE
AEROSPACE
PACKAGING
LOGISTICS
ELECTRONICS
AUTOMATION
SPACE ENGINEERING
ROBOTICS
MEDICAL
COMPOSITES
RAIL
TRANSPORTATION

Pre-register online now for your free entry badge and show preview at **www.industrysouth.co.uk**

SOUTHERN MANUFACTURING & ELECTRONICS is an ETES event organised by European Trade & Exhibition Services Ltd

Tel 01784 880890
email philv@etes.co.uk

etes Regional Manufacturing Exhibitions

Register here with your smartphone

Supported by: fac · CBM Confederation of British Metalforming · Composites UK · BGA British Gear Association · gtma